Oxygen and carbon isotope and Sr/Ca signatures of high-latitude Permian to Jurassic calcite fossils from New Zealand and New Caledonia

Clemens V. Ullmann[a,b*], Hamish J. Campbell[c], Robert Frei[a] and Christoph Korte[a]

[a] University of Copenhagen, Department of Geosciences and Natural Resource Management and & Nordic Center for Earth Evolution (NordCEE), Øster Voldgade 10, 1350 Copenhagen K, Denmark.
[b] University of Exeter, Camborne School of Mines and Environment and Sustainability Institute, College of Engineering, Mathematics and Physical Sciences, Penryn, Cornwall, TR10 9FE, United Kingdom
[c] GNS Science, 1 Fairway Drive, Avalon, Lower Hutt 5010, New Zealand.
*Corresponding author, email: c.v.ullmann@gmx.net Tel.: +44 1326 255721; fax: +44 1326 370450.

Abstract

Calcite fossils from New Zealand and New Caledonia provide insight into the Permian to Jurassic climatic history of Southern High Latitudes (southern HL) and Triassic Southern Intermediate Latitudes (southern IL). These results permit comparison with widely studied, coeval sections in Low Latitudes (LL) and IL. Oxygen isotope ratios of well-preserved shell materials indicate a partially pronounced Sea Surface Temperature (SST) gradient in the Permian, whereas for the Triassic no indication of cold climates in the southern HL is found. The Late Jurassic of New Zealand is characterized by a slight warming in the Oxfordian–Kimmeridgian and a subsequent cooling trend in the Tithonian. Systematic variations in the $\delta^{13}C$ values of southern HL samples are in concert with those from LL sections and confirm the global nature of the carbon isotope signature and changes in the long-term carbon cycle reported earlier.

Systematic changes of Sr/Ca ratios in Late Triassic brachiopods, falling from 1.19 mmol/mol in the Oretian (early Norian) to 0.67 mmol/mol in the Warepan (late Norian) and subsequently increasing to 1.10 mmol/mol in the Otapirian (~Rhaetian), are observed. Also Sr/Ca ratios of Late Jurassic belemnite genera Belemnopsis and Hibolithes show synchronous changes in composition that may be attributed to secular variations in the seawater Sr/Ca ratio. For the two belemnite genera an increase from 1.17 mmol/mol in the Middle Heterian (~Oxfordian) to 1.78 mmol/mol in the Mangaoran (~late Middle Tithonian) and a subsequent decrease to 1.51 mmol/mol in the Waikatoan (~Late Tithonian) is documented.

1. INTRODUCTION

Geochemical information derived from carbonate fossils plays an important role in determining past environmental parameters. Systematic analyses of fossil shell calcite led to Phanerozoic compilations of oxygen and carbon isotope ratios (**Veizer et al., 1999**), $^{87}Sr/^{86}Sr$ ratios (**Veizer et al., 1999**; **McArthur et al., 2001**) and Sr/Ca ratios (**Steuber and Veizer, 2002**). These compilations have improved our knowledge about past environmental conditions. They have refined long-range correlations of sedimentary successions and have provided new insight into secular changes in past seawater composition related to tectonic and biological processes (e.g. **Veizer et al., 1999**; **McArthur et al., 2001**; **Steuber and Veizer, 2002**; **Ullmann et al., 2013a**; **Shaviv et al., 2014**). In recent years, large, integrated datasets have been compiled. Compilations covering the whole Phanerozoic now rely on > 16,000 $\delta^{13}C$ and $\delta^{18}O$ values and provide information about separate climatic zones (**Prokoph et al., 2008**).

Whilst such compilations have refined our understanding of the long-term evolution of Earth's surface, they are characterised by a strong bias towards the analysis of materials from low palaeo-latitudes. 87 % of the $\delta^{18}O$ data reported for shelf carbonates by **Prokoph et al. (2008)** comes from low palaeo-latitudes and less than 2 % are from high palaeo-latitudes (>58°). This paucity of deep time data from the high palaeo-latitudes has especially impacted on our ability to provide stronger constraints on global greenhouse climates. The high latitudes (HL) respond more strongly to subtle climate change than the tropical realm (**Holland and Bitz, 2003**). Furthermore, the lack of HL data prevents characterization of important parameters such as latitudinal temperature gradients and high latitude faunal assemblages. For a more complete understanding of environmental conditions in deep time, it is therefore critical to target high latitude sites (**Dera et al., 2011**).

Zealandian sedimentary successions were situated in high (> 60°S) latitudes in the case of New Zealand and in intermediate (30 – 60°S) latitudes in the case of New Caledonia throughout the Permian to Jurassic (**Adams et al., 2007**; **Stevens, 2008**). Zealandia therefore represents a key region for investigating high latitude climates of the past. It is characterised by a long-lasting stable tectonic setting (**Mortimer, 2004**), promising a reliable geochemical record through this time interval, but Palaeozoic and Mesozoic geochemical data are sparse for Zealandian sediments. Only sections of major boundary events and the Late Jurassic have been studied in detail (e.g. **Stevens and Clayton, 1971**; **Podlaha et al., 1998**; **Krull et al., 2000**; **Gröcke et al., 2003**). To improve our understanding of Permian to Jurassic climate in this important region, we report the stable carbon and oxygen

isotope composition, [87]Sr/[86]Sr ratios as well as Sr/Ca and Mn/Ca ratios of fossil shell materials of New Zealand and New Caledonia. These data provide a 150 myr record isotope and Sr/Ca trends for the southern HL and inform about changes in the pole-to-equator distribution of major climatic zones and associated temperature gradients for the Permian to Jurassic. Our Sr/Ca ratio dataset generated from best preserved samples also appends the currently small database for Permian, Triassic and Late Jurassic fossil Sr/Ca ratios.

2. REGIONAL SETTING

The geochemical data presented herein are derived from the analysis of shelly marine invertebrate fossils collected from well-known mapped formations and localized outcrops from New Zealand (Brook Street and Murihiku Terranes) and New Caledonia (Téremba Terrane; **Figs. 1-3**).
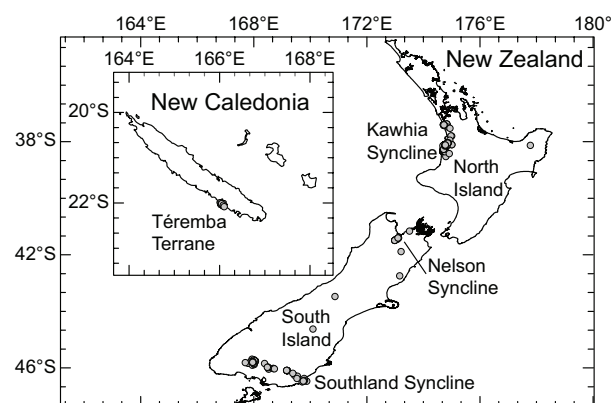

Fig. 1: Sample locations in New Zealand and New Caledonia (inset).

2.1 Palaeogeography and plate tectonic evolution

The Brook Street and Murihiku Terranes originated in a more or less autochthonous relationship ocean-ward of the Median Batholith, a long-lived Devonian to Cretaceous magmatic complex on the South-eastern margin of Gondwana. Within New Zealand, the Murihiku Terrane is the least deformed and stratigraphically most coherent basement terrane. The same can be said of the Téremba Terrane within New Caledonia. It has been shown that, for all intents and purposes, the latter two terranes

are equivalents of each other but they represent different segments of an elongate volcanic arc basin flank complex that developed along an active subduction margin of Gondwana (**Hudson, 2000, 2003**). Today, these two terranes are oriented more or less North-South and occupy markedly different latitudinal settings: New Zealand between 46 and 37°S, and New Caledonia between 23 and 20°S.

The Permian (Brook Street Terrane), Late Permian-Jurassic Murihiku Supergroup (Murihiku Terrane) fore-arc volcaniclastic sequences of New Zealand and correlative Baie de St Vincent Group (Téremba Terrane) of New Caledonia (**Fig. 3**) represent inner shelf to bathyal environments and are relatively fossil-rich. These fossils are the basis of the well-established 'local' New Zealand biostratigraphic zonal scheme which has been correlated with the international geological time scale. These correlations are based on common cosmopolitan fossil bio-events (first appearance datums and last appearance datums) using specific fossil taxa, mainly molluscs, including bivalves, ammonoids and ammonites. A concise summary of the New Zealand geological timescale and its chronostratigraphic calibration and limitations is provided by **Cooper et al. (2004)** and **Raine et al. (2015)**.

During the Permian to Jurassic, the shallow to deep marine successions deposited in the vicinity of Antarctica and Australia are believed to have been situated at high palaeolatitudes (**Fig. 2**). Based on plant fossil assemblages (**Pole, 2009**) and sedimentary provenance studies (**Adams et al., 2007**) it has been suggested that New Zealand terranes may even have been situated beyond the Southern Polar circle (**Zharkov and Chumakov, 2001**; **Stevens, 2008**; **Torsvik and Cocks, 2013**). For New Caledonia **Adams et al. (2007)** estimate a palaeoposition close to Australia in the southern IL for the Late Triassic. It is assumed that our study area was situated in a stable plate tectonic setting throughout the Late Palaeozoic and much of the Mesozoic (**Mortimer, 2004**). In the Cretaceous, a change in the tectonic setting led to the migration of the arc, ceasing subduction at the southeastern Gondwana margin, and subsequent extension that terminated the Austral Megasequence and started the Zealandia Megasequence (**Mortimer et al., 2014**). This extensional phase began about 105 myr ago and led to the opening of the Tasman Sea, separating the Zealandian crustal fragments from the Gondwana margin (**Collot et**
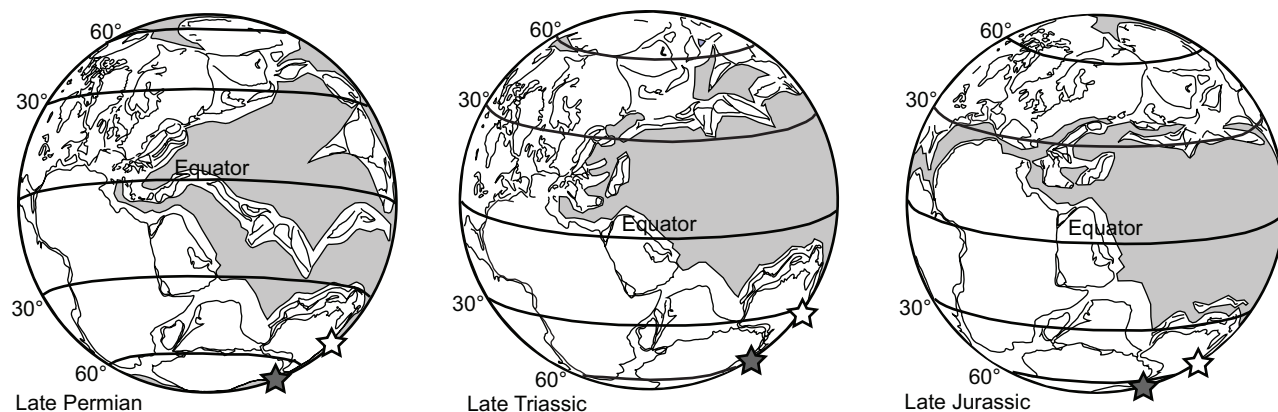

Fig. 2: Palaeogeographic reconstructions for the Late Permian, Late Triassic and Late Jurassic, modified after **Stampfli and Borel (2002)**. The grey star marks the approximate position of the Brook Street and Murihiku terranes (New Zealand) and the white star shows the approximate position of the Téremba Terrane (New Caledonia).
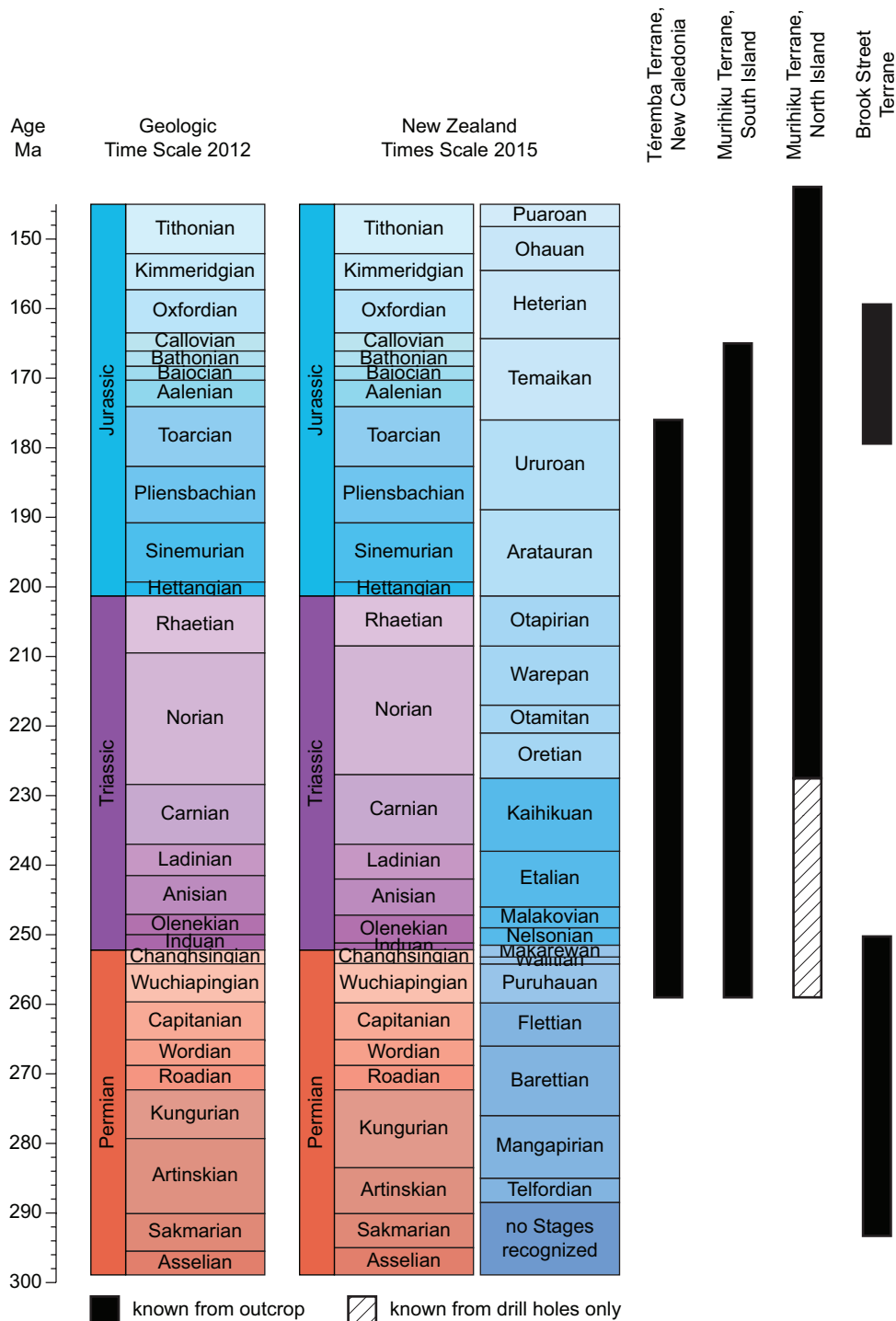
Fig. 3: Permian to Jurassic part of the Geologic Timescale after **Gradstein et al. (2012)** and New Zealand Timescale with correlation to global time scale after **Raine et al. (2015)**. Stratigraphic ranges of investigated terranes are indicated as bars.

al., 2009). The subsequent evolution of the Zealandian successions follows a first order transgressive-regressive cycle: separation (Momotu Supergroup), rifting and formation of the Tasman Sea (Haeranga Supergroup), maximum marine inundation (Waka Supergroup), regression and widespread emergence (Maui and Pakihi Supergroups) (**Mortimer et al., 2014**).

Major displacement, shearing and uplift of the Austral Superprovince rocks is related to the Tertiary formation of the Alpine Fault, constituting the boundary of the Australian and Pacific Plates (**Cooper et al., 1987**; **Kamp et al., 1989**; **Sutherland, 1999**). Exposure of the New Cal-

edonian Téremba Terrane is related to Eocene obduction (**Cluzel et al., 2012**).

2.2 Investigated terranes

The sedimentary successions studied here are part of the Austral Superprovince of Zealandia, comprising the Zealandian crystalline rocks and sedimentary rocks of Gondwanan origin, whose geologic evolution is described in detail in **Mortimer et al., (2014)**.

Brook Street Terrane rocks of the Permian Productus Creek Group are structurally complex, fossiliferous plat-

form sediments formed in a volcanic island arc setting (**Landis et al., 1999**; **Mortimer et al., 1999**; **Spandler et al., 2005**; **Adams et al., 2007**). The Productus Creek Group yields the richest and best preserved shelly brachiopod faunas of Middle to Late Permian age in New Zealand. This succession is restricted to a small area east of the Takitimu Mountains in Southland, South Island (**Turnbull and Allibone, 2003**). Permian outcrops of the > 500 m thick sequence of the Productus Creek Group examined in this study are from the Southland Syncline (**Spörli, 1978**, **Fig. 1**).

In New Zealand, the Murihiku Terrane occurs structurally between the Early Permian to Middle Jurassic Brook Street Terrane (to the West) and the Late Permian to Middle Triassic Dun Mountain – Maitai Terrane (to the East). Murihiku Terrane sediments of the Murihiku Supergroup were deposited during the Late Permian to Early Cretaceous (**Campbell et al., 2003**; **Adams et al., 2007**). The volcanic arc that produced the original Murihiku Supergroup sediments and tuffs is largely eroded away but is interpreted to have been located within the Median Batholith (to the west of the Brook Street Terrane) and is represented today by plutonic remnants preserved in places, for instance, in Stewart Island and the Foveaux Strait coast of Southland. The Murihiku Supergroup comprises mostly marine sediments with a diverse and relatively rich fossil record. These sediments are dominated by siltstone, sandstone and tuff and subordinate conglomerate, shell beds, whereas limestones, cherts and black shales are absent (**Campbell et al., 2003**). Regressive phases leading to terrestrial sedimentation of coarse-grained sandstones and gravels with abundant plant material are recorded for the Middle Jurassic (**Hudson, 2000**). The thickness of Upper Permian to Lower Cretaceous strata reaches at least 17.5 km, with an especially thick Upper Jurassic succession testifying to rapid sedimentation of volcaniclastic material during this time (**Campbell et al., 2003**; **Kear and Motimer, 2003**). The Triassic succession in the Murihiku Supergroup has been subdivided into local series and stages as follows from oldest to youngest: The Early to Middle Triassic (Induan to Ladinian) Gore Series: Nelsonian, Malakovian, Etalian, Kaihikuan stages; and the Late Triassic (Carnian to Rhaetian) Balfour Series: Oretian, Otamitan, Warepan, Otapirian stages. Detailed biostratigraphic research has recognised a number of major disconformities within the Triassic (**Campbell et al., 2003**). These disconformities coincide with the bases of local stages and denote significant non-representation of Triassic time. Norian time is especially well-represented within the Murihiku Supergroup, both in terms of fossils and stratigraphic thickness. The Rhaetian is also well-represented in terms of thickness, but has only moderate fossil diversity. The Jurassic succession is subdivided into the Early Jurassic Herangi Series: Aratauran, Otamitan; the Middle-Late Jurassic Kawhia Series: Temaikan, Heterian, Ohauan; and the Late Jurassic Oteke Series: Puaroan (**Raine et al., 2015**; **Fig. 3**). Specimens from the Murihiku Terrane were derived from outcrops in the Southland and Nelson Synclines of the South Island and the Kawhia Syncline on the North Island of New Zealand (**Campbell et al., 2003**; **Fig. 1**).

The Téremba Terrane of New Caledonia comprises island-arc-derived, volcaniclastic, medium-grained, greywackes of Late Permian to Middle Jurassic age (**Cluzel et al., 2012**). The > 1 km thick deposits of the studied Upper Triassic fossil localities of the Baie de St.-Vincent Group (**Campbell, 1984**; **Campbell and Grant-Mackie, 1984**) have been interpreted to represent forearc deposits in a fully marine, near-shore setting (see **Ullmann et al., 2014a** for further details). The local New Zealand stages are directly applicable to successions of Baie de St Vincent Group in the Téremba Terrane of New Caledonia. Whereas the sequence covers Induan to Kimmeridgian time, its sedimentary strata predominantly represent the Norian to Toarcian. Like the Murihiku Terrane, also the Triassic of the Téremba Terrane is characterized by a thick and fossiliferous Norian and thick Rhaetian with moderate fossil diversity. It also shares the major disconformities coinciding with bases of local stages with the Murihiku Terrane. Samples from the Téremba Terrane were derived from the Baie de St. Vincent area of New Caledonia (**Fig. 1**).

3. MATERIALS AND METHODS

3.1 Samples

To investigate Permian to Jurassic environmental conditions in the southern HL we sampled shell calcite of brachiopods, bivalves and belemnites (n = 1423) from Early Permian to Late Jurassic successions of New Zealand and New Caledonia (**Fig. 1**). With only two exceptions (specimens NZ0138 and NZ0235A), the New Zealand specimens acquired for analyses stem from the Brook Street and Murihiku Terranes. New Caledonia specimens were acquired from the Téremba Terrane. Neither specimen NZ0138 (Rakaia Terrane) nor specimen NZ0235A (Caples Terrane) passed the screening for diagnetic overprints and these terranes are therefore not introduced in further detail.

A subset of the fossil specimens analysed here was assembled during field work in November and December 2010 on the North and South Islands of New Zealand. Most of the material was sampled, however, from bulk and reference collections held at the University of Auckland, GNS Science and the University of Otago. All sampled localities are recorded in the Fossil Record Electronic Database (FRED) which is jointly owned and operated by the Geoscience Society of New Zealand and GNS Science. Essential information for the fossil localities sampled is given in **Supplementary Table 1** and meta data for the localities including information on age assignments can be retrieved via the FRED (**http://www.fred.org.nz/**)

3.2 Sampling routines

Geochemical signatures in fossil shell materials are often found to be partially reset due to post-depositional alteration, demanding careful optical and chemical examination of the fossil shells before palaeoenvironmental

interpretation of the data (**Ullmann and Korte, 2015**).

3.2.1 Scanning electron microscopy

All samples were checked for preservation by optical microscopy. For each specimen a flake of approximately 1 x 1 mm size was mounted on a stub for Scanning Electron Microscopy (SEM, **Fig. 4**). The shell fragments were gold-coated before introduction into the SEM. All investigations were carried out using the FEI Quanta 250 SEM at the Geological Museum in Copenhagen in high vacuum mode.
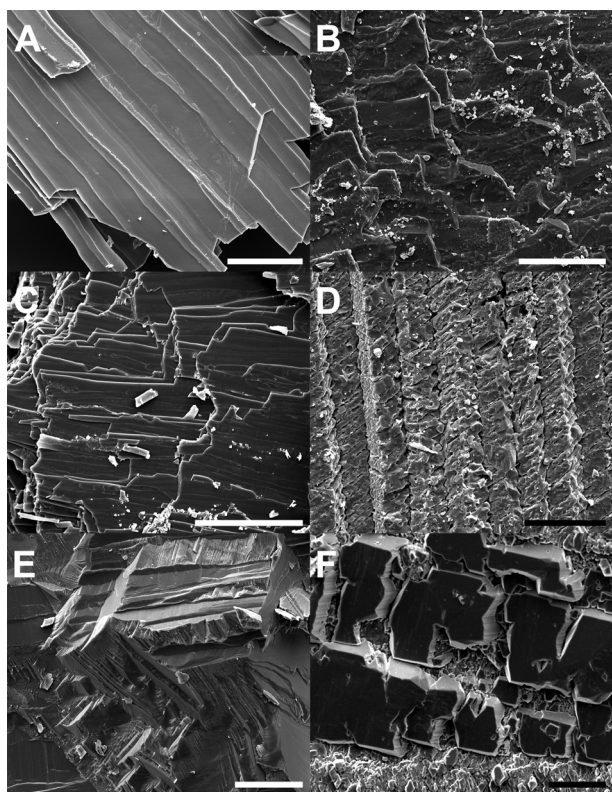

Fig. 4: SEM photographs of different fossil shell materials. Scale bars are 50 µm. A: well-preserved Temaikan (Middle Jurassic) brachiopod shell (NZ0110D). B: recrystallized Aratauran (Early Jurassic) brachiopod shell (NZ0107B). C: well-preserved Flettian (Middle Permian) bivalve shell (NZ0207B). D: recrystallized Early Permian bivalve shell (NZ0219). E: well-preserved Ohauan (Late Jurassic) belemnite rostrum (NZ0264C). F: Puaroan (Late Jurassic) belemnite rostrum (NZ0033E) showing significant recrystallization and dissolution.

3.2.2 Sampling of fossil calcites

Brachiopods were sampled with a stainless steel needle. The topmost shell layers were detached in order to avoid contamination with slightly altered parts of the shell and attached sediment. Because vital effects in the primary layers of brachiopods may lead to isotopic disequilibrium (e.g. **Carpenter and Lohmann, 1995**; **Auclair et al., 2003**; **Parkinson et al., 2005**; **Cusack et al., 2008**; **Yamamoto et al., 2010**) we targeted only secondary layers for preparation. Similarly, bivalve shell fragments were prepared for analysis with a stainless steel needle after cleaning the shell surface by scraping off the top layers. Belemnites were prepared using an electronic hand drill equipped with a diamond sintered cylindrical drill bit with a diameter of ~0.8 mm. Samples were taken from translucent, brownish calcite of the rostra. Owing

to likely alteration (e.g. **McArthur et al., 2007**; **Li et al., 2012**; **Ullmann et al., 2013b**) apical line and rims as well as very pale, opaque parts were avoided. After cleaning the surface by grinding away the surface with the drill, belemnite samples were prepared either by drilling single holes or traces from the outer growth bands towards the apical line.

3.2.3 Analytical methods

Geochemical analyses of fossil materials were performed using procedures outlined in **Ullmann et al. (2013b)**. Sample sizes were generally ca. 0.6 mg for combined $\delta^{13}C$, $\delta^{18}O$ and trace element analyses. For carbon and oxygen isotope analyses using the IsoPrime Gas Source Isotope Ratio Mass Spectrometer at the University of Copenhagen, protocols for continuous flow stable isotope analyses described in **Spötl and Vennemann (2003)** were adopted with adjustments due to laboratory specifications. The accuracy of the method was checked by multiple preparation and measurement of the international reference materials NBS-18 and NBS-19, as well as laboratory reference materials from the Freie Universität Berlin. The long-term (2sd) reproducibility of this method, as determined from the measurements of the in-house reference material "LEO" (Carrara Marble) in 2011, is 0.08 ‰ for $\delta^{13}C$ and 0.18 ‰ for $\delta^{18}O$ (n = 649). Trace element concentrations were determined from the reacted carbonate remains that were used for stable isotope analyses, employing routines analogous to those described by **Coleman et al. (1989)** with an Optima 7000 DV ICP-OES from Perkin Elmer at the University of Copenhagen. The reproducibility (2sd) for the reference materials JDo-1 (n = 190) and JLs-1 (n=266) was better than 2.4 % for Sr/Ca. Reproducibility (2sd) for Mn/Ca in JDo-1 (n = 190) was 2.8 % and 8 % in JLs-1 (n = 266), with the higher uncertainty of the latter owing to its low Mn/Ca ratios of ~29 µmol/mol. The analytical bias for the element/Ca ratios, determined by the deviation of the mean results for JDo-1 and JLs-1 from the values given by **Imai et al. (1996)**, is smaller than 2 %. Typical limits of quantification were 1.3 µmol/mol for Sr/Ca ratios and 5.5 µmol/mol for Mn/Ca ratios.

$^{87}Sr/^{86}Sr$ ratios were determined for a sub-set of samples that was chosen according to material availability, coverage of the studied interval of time, as well as textural and chemical preservation markers. An average of 2.3 mg calcite was dissolved in 1 M HCl with a sample to acid ratio of 1 mg/ml. 0.5 ml of the resulting solution was used for trace element concentration measurement, the rest was taken for strontium purification. After drying on a hotplate at 80°C the residues were re-dissolved in ~0.2 ml of 3 M nitric acid. The strontium was purified with 3 M HNO_3 using Sr-Spec resin (**Horwitz et al., 1992**) with EppendorfTM pipette tips (1 ml) - equipped with a filter - as ion exchange columns. Purified strontium was eluted with de-ionized water and, after the addition of about 25 µl of 0.1 M H_3PO_4 and a subsequent drying at 80°C, loaded on single rhenium filaments in 5 µl of Ta_2O_5-H_3PO_4 matrix. $^{87}Sr/^{86}Sr$ ratios were measured with a VG 54 Sector TIMS with 8 Faraday cups in dynamic multi-collection mode at the University of Copenhagen.

Instrumental fractionation was corrected for by using an exponential law. The repeatability of the method was found to be 0.000018 (2 sd, n=18). Accuracy and precision of the measurements were checked by multiple measurements of the reference material NISTSRM 987 giving a mean $^{87}Sr/^{86}Sr$ ratio of 0.710243 ± 0.000022 (2 sd, n = 15).

3.2.4 Preservation of geochemical signatures

To assess further the quality of preservation of the fossil shells analyzed we examined their Mn/Ca ratios. Mn is found to be enriched in fossil carbonates that have experienced post-depositional alteration (e.g. **Brand and Veizer, 1980**; **Al-Aasm and Veizer, 1982**; **Veizer et al., 1986**; **Brand, 1989**; **Denison et al., 1994**). Mn concentrations have therefore been widely applied as a quality indicator of fossil carbonates (e.g., **Voigt et al., 2003**; **Korte et al., 2005a,b, 2008**; **Wierzbowski and Joachimski, 2007**; **Nunn and Price, 2010**; **Ullmann et al., 2013a,b**).

In Late Triassic brachiopods from New Caledonia, Mn enrichments are associated with trends towards very negative $\delta^{13}C$ values (down to ~-21 ‰), negative $\delta^{18}O$ values (down to ~-13 ‰), unradiogenic $^{87}Sr/^{86}Sr$ ratios and lower Sr/Ca ratios (**Ullmann et al., 2014a**). In the Late Jurassic succession around Kawhia (North Island, New Zealand), enrichments in Mn are associated with moderately low $\delta^{13}C$ values (down to ~-3 ‰), negative $\delta^{18}O$ values (down to ~-12 ‰), unradiogenic $^{87}Sr/^{86}Sr$ ratios and a lowering of Sr/Ca ratios (**Ullmann et al., 2013b**).

Common limits for Mn concentrations are 250 µg/g for brachiopods and bivalves (**Korte et al, 2005a**; **Korte and Hesselbo, 2011**) and 100 µg/g for belemnites (**Price and Mutterlose, 2004**; **Nunn and Price, 2010**). The use of static Mn limits is complicated by spatial and temporal geochemical variability of diagenetic fluids (**Ullmann et al., 2013b, 2014**). Furthermore, it is possible that primary Mn uptake is significant during biomineralization in settings with significant freshwater contributions (e.g. **Almeida et al., 1998**; **Vander Putten et al., 2000**) and/or dysoxic water masses (**Korte and Hesselbo, 2011**). Samples showing such primary enrichment would, however, in most instances not represent fully marine conditions. In order to avoid interpreting data in our records that are affected by post-depositional alteration and effects of marginal settings, we therefore adopt strict limits of Mn/Ca < 0.20 mmol/mol for bivalves and brachiopods (**Ullmann et al., 2014a**) and Mn/Ca of < 0.10 mmol/mol for belemnites. Samples with intermediate degree of preservation (Mn/Ca ratios up to 0.45 mmol/mol) are shown in the figures with differing color code but are not used for further calculations. Results for samples with Mn/Ca > 0.45 mmol/mol are not further discussed in terms of palaeoenvironmental implications but all data generated are provided online in **Supplementary Table 2**.

3.2.5 Presentation of the data

Most of the Permian to Late Triassic data was measured on brachiopods, whereas the Late Jurassic values are chiefly from belemnites. Only very few bivalves were found to be sufficiently well preserved to be incorporated into the dataset and are therefore not discussed in detail. In order to derive a long-term trend for the high palaeolatitudes with acceptable statistical certainty and robust age assignment, the New Zealand Stages and Substages have been chosen as a timeframe (**Figs. 5-8**). This temporal resolution also honours the fact that age assignment of many of the studied fossil localities is limited to the New Zealand Stage level. Correlations of the New Zealand Stages to the International timescale are from **Raine et al. (2015)**. **Figures 6-7** illustrate $\delta^{13}C$ and $\delta^{18}O$ data derived from brachiopod and belemnite calcite, with the brachiopod data differentiated into New Zealand and New Caledonia samples. Samples with Mn/Ca ratios indicating very good preservation (< 0.20 mmol/mol for brachiopods and < 0.10 mmol/mol for belemnites) are plotted together with samples showing Mn/Ca ratios indicative of good preservation (Mn/Ca > 0.20/0.10 mmol/mol and < 0.45 mmol/mol). Average values are only calculated from samples classified as very well-preserved and only for intervals for which at least ten such samples are available. Data from the IL are presented together with HL data but with differing colour code. Only $\delta^{13}C$, $\delta^{18}O$ and Sr/Ca data from very well-preserved samples are described and discussed below in detail and it is pointed out specifically when data from other samples are integrated in description and/or discussion.

4. RESULTS

4.1 $^{87}Sr/^{86}Sr$ ratios

$^{87}Sr/^{86}Sr$ ratios measured for fossil localities of New Zealand and New Caledonia are shown in **Figure 5** (see also **Supplementary Table 3**). The three values obtained for Permian brachiopods of the Brook Street Terrane (South Island) (**Fig. 5**) all show comparatively low $^{87}Sr/^{86}Sr$ ratios of 0.706784 to 0.706855. $^{87}Sr/^{86}Sr$ ratios of Triassic brachiopods of the Murihiku and Brook Street Terranes (South Island) are more radiogenic and fall into the range of 0.707551 to 0.707774, and $^{87}Sr/^{86}Sr$ ratios of the Late Triassic of New Caledonia are even more radiogenic (0.707749 to 0.707958). One Middle Jurassic $^{87}Sr/^{86}Sr$ ratio from a belemnite of the Murihiku terrane shows a value of 0.707058, and during the Late Jurassic a general increase of ratios from 0.706838 to 0.707135 is observed in Murihiku belemnites.

4.2 $\delta^{18}O$ values

4.2.1 Permian-Triassic brachiopod data

The oxygen isotope composition of brachiopod shells from the Permian to Jurassic of New Zealand and New Caledonia is plotted in **Figure 6**. During the Early Permian, three brachiopod oxygen isotope values vary in the range of -1.1 to -0.1 ‰. Compared with the Early Permian, higher variability amounting to a range of 3 ‰ and values as light as -2.5 ‰ are observed in the Middle Permian. The Late Permian Puruhauan Stage (~Wuchiapingian) is characterized by $\delta^{18}O$ values significantly lower

than in the previous Stages (-2.5 to -1.3 ‰; **Fig. 6**).

Only negative oxygen isotope values are recorded in the HL fossil calcite from brachiopods of latest Permian to Late Triassic age. Kaihikuan (late Ladinian - Carnian) values of the Brook Street Terrane range from -4.8 to -1.4 ‰ (n = 59) and three values from the Murihiku Terrane fall in the range of -5.7 to -2.3 ‰. During the following Oretian Stage (early Norian) 18 values from the Murihiku Terrane span an interval from -6.1 to -3.9 ‰, with a single value at -1.2 ‰. 22 Otamitan (middle Norian) values from the Murihiku Terrane generally range from -5.0 to -1.7 ‰ with two very negative values of -7.6 and -6.9 ‰. Three well-preserved Warepan (late Norian) samples from the Murihiku Terrane show values from -2.6 and -2.0 ‰. Otapirian (~Rhaetian) values from the Murihiku Terrane range from -5.0 to 0.0 ‰ (n = 6).

IL brachiopod samples (New Caledonia) are available from the Oretian (early Norian), Warepan (late Norian) and Otapirian (~Rhaetian) Stages (**Fig. 6**). A single Oretian value of -4.2 ‰ is on the heavy side of values observed in the HL. Warepan values of -3.0 to -1.2 ‰ (n = 7) are more variable, but compatible with HL values of the same age. Also for the Otapirian IL values of -1.3 to -4.7 ‰ (n = 44) compare well to HL values.

Average HL $\delta^{18}O$ values for the Triassic Stages for which 10 or more data points are available decrease from -2.9 ± 0.3 ‰ (2err, n = 62) in the Kaihikuan (~ late Ladinian - Carnian) Stage to -4.9 ± 0.5 ‰ (2err, n = 18) in the Oretian (early Norian) Stage (**Fig. 6**). This negative shift is followed by an increase to -3.8 ± 0.6 ‰ (2err, n = 22) in the Otamitan (middle Norian). A continuation of this increasing trend is indicated by comparatively positive HL and IL isotope values in the Warepan (late Norian)

and an average of -2.5 ± 0.3 ‰ (2err, n = 44) for the IL in the Otapirian (~Rhaetian) Stage.

4.2.2 Jurassic belemnite data

Apart from two lower Temaikan (~Aalenian) brachiopod values and two middle Temaikan (~Bathonian) belemnite values, the Jurassic part of the dataset is confined to Late Jurassic belemnite data from the Murihiku Terrane. Three lower Heterian (~ Oxfordian) data points show values between -1.6 and -0.6 ‰. In the middle Heterian (~ Oxfordian), more variable values of -4.1 to +0.8 ‰ are observed (n = 13) and upper Heterian (early Kimmeridgian) data range from -1.3 to + 0.5 ‰ (n = 10). Following lower Ohauan (late Kimmeridgian) data (-3.0 to +0.4 ‰, n = 10) are more negative and more variable than upper Ohauan (early Tithonian) values of -1.3 to +0.8 ‰ (n = 19).

Apart from the lower Ohauan Substage, which shows a light average $\delta^{18}O$ value of -1.5 ± 0.7 ‰ (2 err, n = 10), average belemnite values in the Late Jurassic Substages are compatible with a mean value of -0.5 ‰. This mean value is significantly more positive than Triassic brachiopod values and comparable to Permian values.

4.3 $\delta^{13}C$ values

4.3.1 Permian-Triassic brachiopod data

$\delta^{13}C$ values from three well-preserved Early Permian brachiopod samples fall in the narrow range of +2.9 to +3.5 ‰ (**Fig. 7**). From the Middle Permian, an increasing trend from similar Barettian-Flettian (Kungurian - Capi-
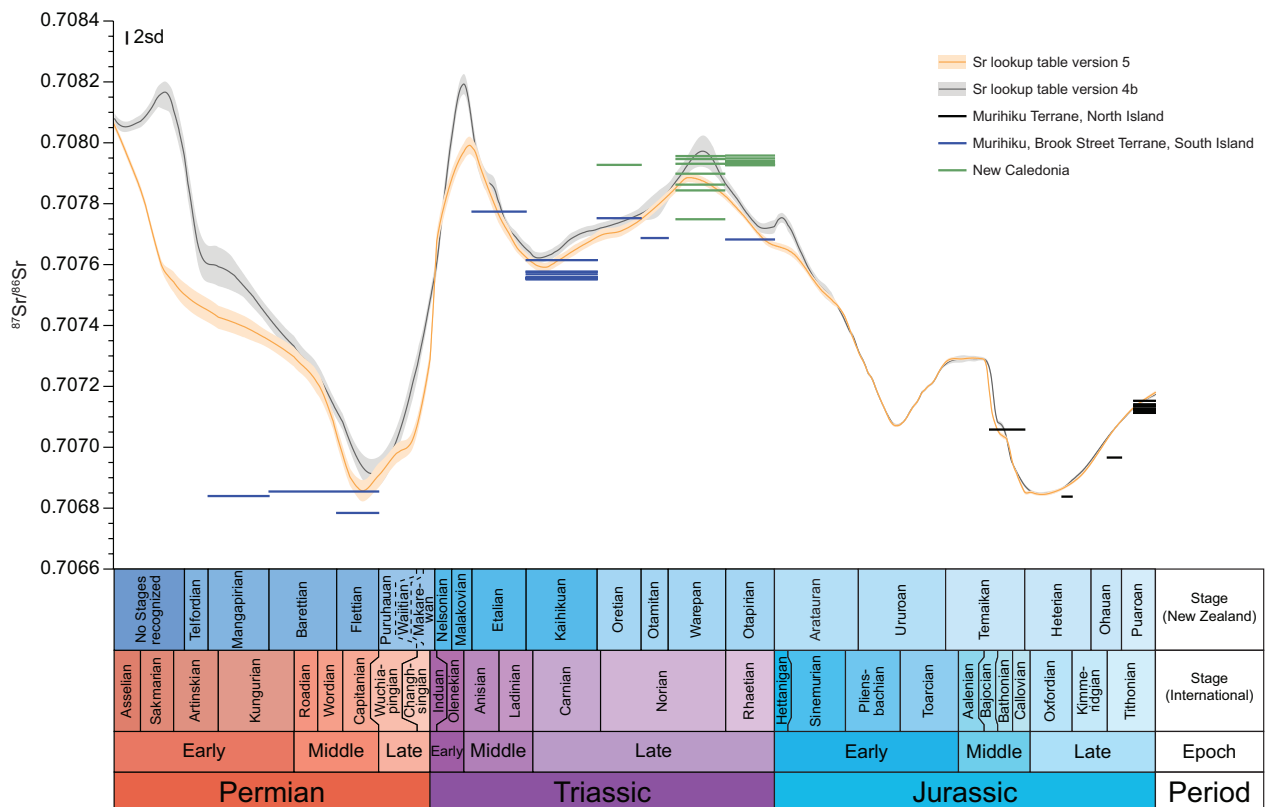

Fig. 5: $^{87}Sr/^{86}Sr$ composition of shell materials plotted against the reference curve from **McArthur et al. (2001)** adjusted to New Zealand and International time scales as correlated in **Raine et al. (2015)**. Red and blue curves show upper and lower confidence intervals, respectively. Black bars: Murihiku Terrane, North Island, New Zealand; Blue bars: Murihiku and Brook Street Terranes, South Island, New Zealand, green bars: New Caledonia.

tanian) values of +2.7 to +4.6 ‰ (excepting a single value of +0.2 ‰) is observed that reaches values of +4.3 to +6.2 ‰ in the Puruhauan (~Wuchiapingian) Stage. This Puruhauan maximum constitutes the highest absolute (+6.2 ‰) and average (+5.6 ‰, n = 7) values observed in the studied time interval (**Fig. 7**).

A subsequent decrease through the Late Permian (+3.1 to +5.2 ‰, n = 3 in the Makarewan; ~ Changhsingian), continues into the Middle Triassic (Etalian; ~Anisian/Ladinian), where 5 values with intermediate geochemical preservation index fall in the range of +0.3 to +0.7 ‰. In the following Kaihikuan (~Carnian) Stage $\delta^{13}C$ increases to values of +2.1 to +5.4 ‰ and an average of +4.3 ± 0.2 ‰ (2 err, n = 62). For the Oretian to Otapirian (Norian - Rhaetian) interval for which HL and IL data are available, the $\delta^{13}C$ values of both latitudinal belts overlap (Fig. 7) and are thus discussed together. The Oretian to Warepan (~Norian, Late Triassic) interval is characterized by decreasing $\delta^{13}C$ values of +3.9 ± 0.8 ‰ (2 err, n = 18) in the Oretian (~early Norian) Stage towards values between +1.9 and +2.1 ‰ in the Otamitan (~middle Norian), Warepan (late Norian) and Otapirian (~Rhaetian) Stages.

4.3.2 Jurassic belemnite data

As for oxygen isotope values, the Early and Middle Jurassic are poorly constrained and data density does not allow for sound interpretations of the trends. Three lower Heterian (~ Oxfordian) data points show values between +1.0 and +1.9 ‰. Middle Heterian (~early Kim-

meridgian) values of +1.8± 0.6 ‰ (2 err, n = 13) for belemnites equal Otapirian (~ Rhaetian) values of brachiopods. The $\delta^{13}C$ values then show a continuous, strong decrease through the late Heterian and Ohauan reaching 2.5 ± 0.6 ‰ (2 err, n = 14) in the Puaroan (~middle - late Tithonian). Towards the Jurassic-Cretaceous transition the $\delta^{13}C$ values show a rebound to more positive values of -0.5 ± 0.4 ‰ (2 err, n = 25) but remain lower than in the pre-Puaroan.

4.4 Sr/Ca ratios

Average Sr/Ca ratios of Permian to Triassic brachiopod shells from New Zealand and New Caledonia and of Late Jurassic belemnite rostra from New Zealand are shown in **Fig. 8**. Too few data are available to robustly constrain Permian brachiopod Sr/Ca ratios at the Stage level. Permian brachiopods with Mn/Ca ratios below 0.2 mmol/mol in the Permian range from 0.57 to 1.26 mmol/mol, with an average of 0.95 ± 0.11 mmol/mol (n = 19). Slightly lower values of 0.74 to 0.88 mmol/mol (n = 3) are encountered for the Permian-Triassic transition (Makarewan; Changhsingian - Induan).

After a data gap in the Early and Middle Triassic, brachiopod Sr/Ca ratios of the Kaihikuan (~ late Ladinian - Carnian) are significantly higher than in the Permian (1.19 ± 0.06 mmol/mol; 2err, n = 48). The remainder of the Triassic is then characterized by a long-term decline in brachiopod Sr/Ca ratios to 0.67 ± 0.14 mmol/mol (2err, n = 10) in the Warepan (late Norian) Stage. Towards the end of the Triassic the Sr/Ca ratios increase again to 1.10
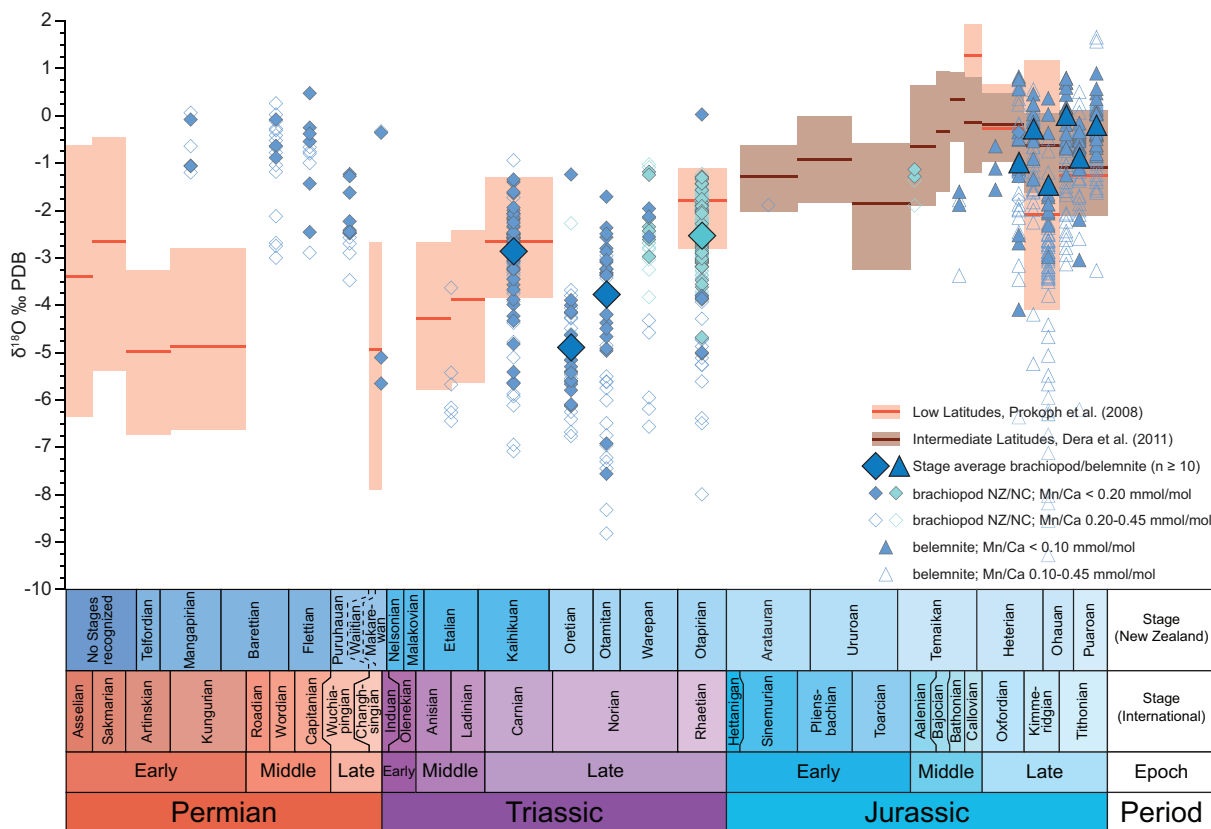

Fig. 6: Oxygen isotope composition of fossil shells from New Zealand and New Caledonia in blue and white. Diamonds: brachiopods; Triangles: belemnites. Large Dark Blue: averages for Stages (and Substages, where stratigraphic subdivision is robust and data density sufficient). Blue: brachiopod samples with Mn/Ca < 0.2 mmol/mol and belemnite samples with Mn/Ca < 0.1 mmol/mol. White: brachiopod samples with Mn/Ca between 0.2 and 0.45 mmol/mol; belemnite samples between 0.1 and 0.45 mmol/mol. The pale red curve for LL is taken from **Prokoph et al. (2008)** and the dark red curve for IL from **Dera et al. (2011)**. New Zealand and International time scales are from **Raine et al. (2015)**.

± 0.07 mmol/mol (2err, n = 53).

Belemnite Sr/Ca ratios of the Late Jurassic are generally higher than Sr/Ca ratios of Triassic and Permian brachiopods and rise from 1.17 ± 0.05 mmol/mol (n = 13) in the Middle Heterian (late Oxfordian) to 1.78 ± 0.04 mmol/mol (n = 14) in the Mangaroan (middle Tithonian). The latest Jurassic Sr/Ca ratios (Waikatoan ~ late Tithonian) are slightly lower with a mean of 1.51 ± 0.06 mmol/mol (n = 25).

5. DISCUSSION

The absolute values and the variability of geochemical proxies differ between individual Stages. The observed heterogeneity of the dataset is controlled by climate and carbon cycle perturbations occurring over sub-stage intervals which cannot currently be resolved because of lacking stratigraphic control for the dataset (see also **Veizer et al., 1999**). In addition to environmental and carbon cycle changes, potentially different habitats, vital effects, and unidentified partial post-depositional alteration of the analyzed specimens contribute to the recorded variability. The subsequent discussion consequently focuses mainly on long-term trends of the newly generated geochemical data set.

5.1. $^{87}Sr/^{86}Sr$ ratios

The Permian and Triassic results generally show a good fit to the marine Sr isotope curve (**Fig. 5**; Look-Up Table Version 4: 08/ 04, and Version 5; **Howarth and**

McArthur, 1997; **McArthur et al., 2001**; see also **Jones et al., 1994**, **Podlaha et al., 1998**; **Korte et al., 2003, 2006**). This part of the reference curve has been subject to considerable change with the current Version 5 listing significantly lower $^{87}Sr/^{86}Sr$ ratios than the previous version (**Fig. 5**). Diagenesis in Late Triassic brachiopod calcite from the Île Hugon and Île Ducos (Baie de St Vincent) area of New Caledonia is found to result in strongly decreasing $^{87}Sr/^{86}Sr$ ratios (**Ullmann et al., 2014a**). The same can be suggested for the Permian-Triassic calcite fossils from New Zealand considering the unradiogenic Sr isotope composition of Permian and Triassic volcaniclastic sedimentary rocks of the Brook Street and Murihiku Terranes (**Adams et al., 2002**). When compared to the current Version 5 of the look-up table, all New Caledonian values apart from three appear to be too radiogenic to be compatible with an Early Triassic age, whereas a much better fit with the previous Version 4 is observed (**Fig. 5**). One fossil locality with an incompatibly high $^{87}Sr/^{86}Sr$ ratio (NC/f0003) lies in the Moindou-Téremba area. The locality is situated about 60 km NW of the other investigated New Caledonian fossil localities from the Île Hugon and Île Ducos (Baie de St Vincent) area and likely experienced a slightly differing diagenetic history. Without a viable source for radiogenic Sr in the Baie de St Vincent sediments of New Caledonia, the look-up table Version 4 is therefore preferred as comparison for Late Norian and Rhaetian $^{87}Sr/^{86}Sr$ ratios.

Middle and Late Jurassic belemnite data of the Murihiku Terrane are in very good agreement with the marine strontium isotope reference curve, which itself is
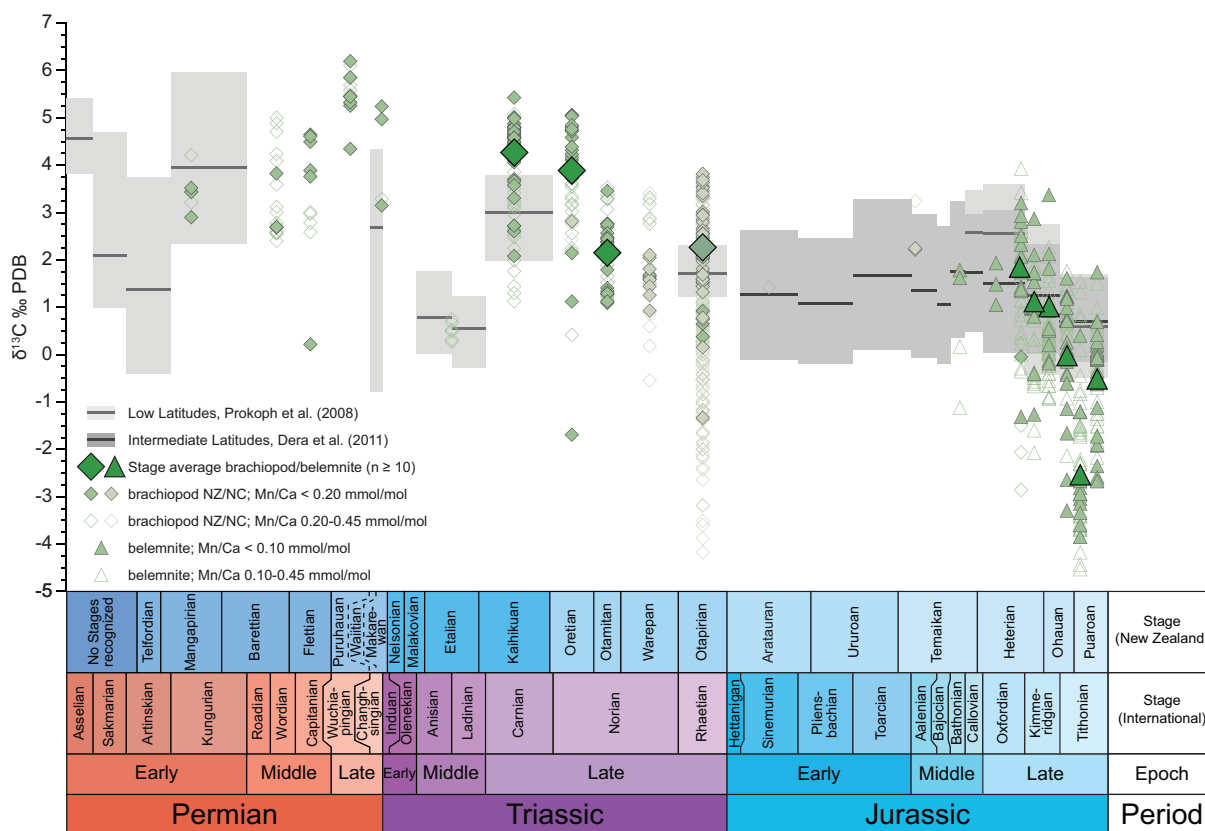

Fig. 7: Carbon isotope composition of fossil shells from New Zealand and New Caledonia in green. Diamonds: brachiopods; Triangles: belemnites. Dark Green: averages for Stages/Substages. Pale Green: brachiopod samples with Mn/Ca < 0.2 mmol/mol and belemnite samples with Mn/Ca < 0.1 mmol/mol. Small symbols: brachiopod samples with Mn/Ca between 0.2 and 0.45 mmol/mol; belemnite samples between 0.1 and 0.45 mmol/mol. The pale grey curve is taken from **Prokoph et al. (2008)** and the dark grey curve from **Dera et al. (2011)**. New Zealand and International time scales are from **Raine et al. (2015)**.

very well defined in this time interval (**Fig. 5**). The few Jurassic data that are incompatible with their assigned age are slightly too unradiogenic, which is in accordance with observed diagnetic trends for the Murihiku Terrane of the North Island (**Ullmann et al., 2013b**).

Otherwise good correspondence of $^{87}Sr/^{86}Sr$ ratios of the New Zealand and New Caledonia samples with the marine Sr isotope reference curve indicates that diagenetic effects on shell geochemistry of samples that have been classified as well-preserved have been minor. Because of measurement uncertainties, significant changes to the marine Sr isotope reference curve and currently unresolvable offsets from the newest reference curve at least for the Late Triassic, further age refinement of the samples employing their $^{87}Sr/^{86}Sr$ ratios is not possible.

5.2. δ18O values

5.2.1. Permian-Triassic brachiopod data

The first identified Stage in New Zealand after the Late Devonian is the Telfordian (Artinskian), which falls into the late phase of the late Palaeozoic ice age (**Korte et al., 2008**; **Isbell et al., 2012**; **Chen et al., 2013**; **Kani et al., 2013**; **Waterhouse and Shi, 2013**; **Limarino et al., 2014**). Throughout the Permian, the new southern HL oxygen isotope values are more positive than those measured for LL brachiopods (**Fig. 6**; **Korte et al., 2005a**), but are comparable or somewhat heavier than those reported for southern HL Australian samples (**Korte et al., 2008**). In the Mangapirian (~Kungurian), for which HL and LL data are available, the observed difference between the two realms is 4.2 ±1.2 ‰ (2err). One Middle Permian brachiopod value of +0.7 ‰ (**Compston, 1960**)

is slightly more positive than the heaviest value observed in the New Zealand dataset (+0.5 ‰). Convergence with low-latitude values is indicated toward the Late Permian as seen in more detail in LL conodont (**Chen et al., 2013**) and brachiopod δ18O (**Korte et al., 2005a**), but the southern HL oxygen isotope data remain more positive than in coeval LL latitude brachiopods, even though sparse sample coverage and large data variability in LL and HL records preclude precise quantification of the offset (**Fig. 6**). Overall, the data are consistent with the high palaeolatitude position of the Brook Street and Murihiku Terranes, south of Tasmania (**Adams et al., 2007**) and confirm the pronounced Permian pole-to-equator temperature gradient observed by **Korte et al. (2008)**. The new data are compatible with a non-glaciated polar Gondwana (**Isbell et al., 2012**), and with generally increasing temperatures in eastern Australia/New Zealand during the Late Permian as inferred from faunal assemblages (**Waterhouse and Shi, 2013**).

The new Triassic oxygen isotope values of HL Zealandian materials show no significant difference between samples from New Caledonia and New Zealand. In contrast to the Permian, the Triassic results are comparable to LL brachiopod data and overlap with LL data in the Kaihikuan (~ Carnian), where an insignificant offset of -0.3 ± 0.4 ‰ (2err) is observed between the two realms (**Fig. 6**). No macrofossil calcite data were previously reported for the Norian low latitudes. As an approximation, whole rock δ18O values – overlapping with fossil data in the late Carnian and Rhaetian (**Korte et al., 2005b**) – indicate relatively stable climatic conditions throughout the Norian. Conodont-derived temperature values from the Lagonegro Basin (Italy) points to a distinct warming in the late Norian (**Trotter et al., 2015**), whereas the
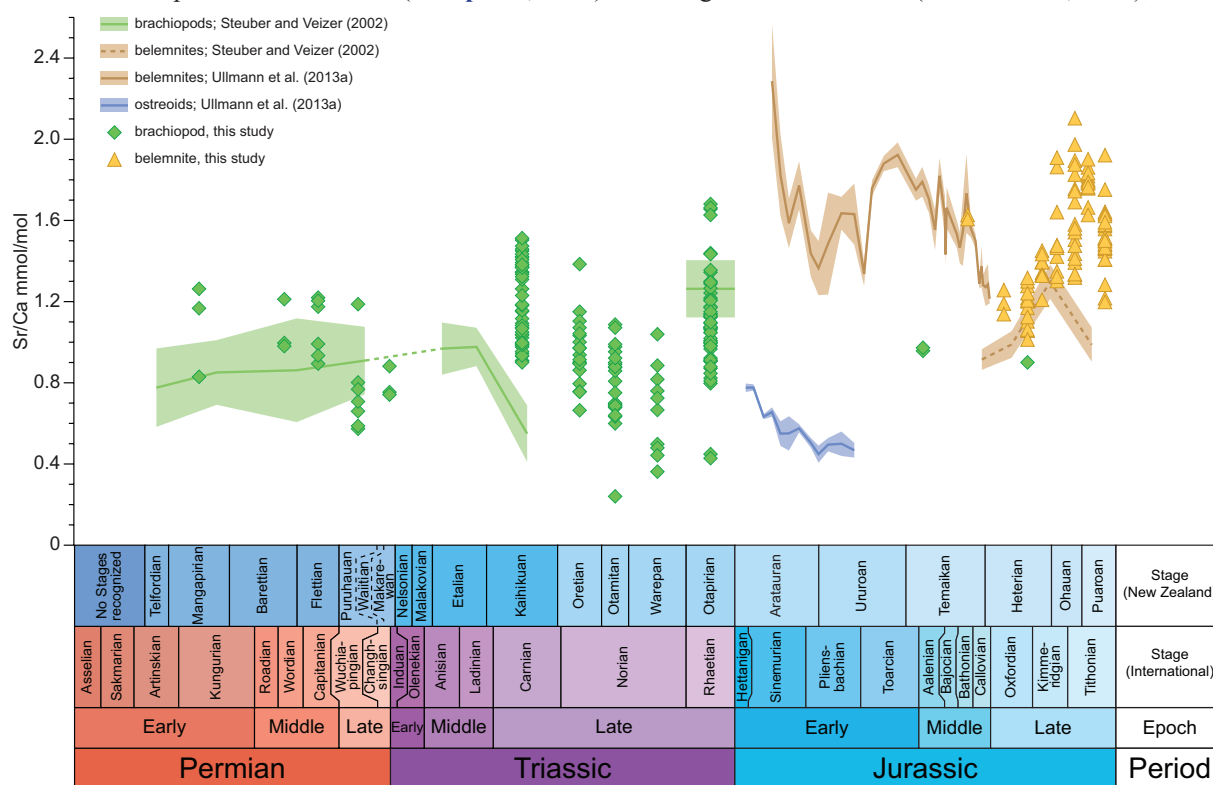

Fig. 8: Sr/Ca ratios of brachiopod samples with Mn/Ca ratios < 0.2 mmol/mol (green diamonds) and belemnite samples with Mn/Ca ratios < 0.1 mmol/mol (orange triangles). The coloured bands show the mean values of the Stages/Substages with 95 % uncertainty (Permian and Triassic brachiopods and Late Jurassic belemnite data recalculated from **Steuber and Veizer (2002)** and Early and Middle Jurassic belemnite and oyster data from **Ullmann et al. (2013a)**).

warmest temperatures in the Zealandian data are found in the Oretian (~ early Norian). Considering the sparsity of available data on this time interval, this disagreement can currently not be resolved.

The similarity of Triassic LL and HL oxygen isotope ratios of macrofossil calcite and the lack of significantly more positive $\delta^{18}O$ values for the Triassic of Zealandia suggest relatively low latitudinal temperature gradients during the Triassic. Temperate to warm climates of HL regions have been inferred in previous studies for Early Triassic (**Kidder and Worsley, 2004**; **Grauvogel-Stamm and Ash, 2005**; **Brayard et al., 2006**; **Preto et al., 2010**; **Retallack et al., 2011**; **Retallack, 2013**), Middle Triassic (**Taylor and Taylor, 1993**; **Cúneo et al., 2003**; **Retallack et al., 2011**; **Retallack, 2013**) and Late Triassic (**Sellwood and Valdes, 2006**), but other studies concluded that considerable latitudinal SST-gradients must have existed at least for parts of the Triassic (**Brayard et al., 2006**; **Zakharov et al., 2009**).

Pervasive partial resetting of the oxygen isotope signature as explanation for our isotopically light southern HL fossil data cannot strictly be ruled out and even the most positive values measured here may have suffered from some post-depositional isotopic exchange. However, $^{87}Sr/^{86}Sr$ ratios of fossils from Triassic localities of the present study are generally compatible with the seawater strontium isotope curve (**Fig. 5**), indicating only minor effects of recrystallization on samples which passed optical and chemical screening for diagenesis. Also diagenetic trends in brachiopods from New Caledonia that affected carbon isotope ratios ~2.5 times stronger than $\delta^{18}O$ values (**Ullmann et al., 2014a**) speak against strong alteration of the HL and IL oxygen isotope signatures. Original $\delta^{13}C$ values would have been extremely heavy if significant diagenetic changes of the $\delta^{18}O$ signatures in our Late Triassic materials had taken place (**Fig. 7**). The observed discrepancies may rather be caused by palaeogeographic differences between the Zealandian fossil localities and the correlative data from the marginal Tethyan Basins (**Korte et al., 2005b**; **Mette et al., 2012**), with generally shallower water depths in the former (**Ullmann et al., 2014a**). Analyses of fossils from other coeval successions would be necessary to clarify the nature of the putative Late Triassic SST gradients.

5.2.2. Jurassic belemnite data

There is an ongoing discussion about the significance of oxygen isotope ratios from belemnite rostra because of their poorly constrained habitats and tendencies to point to relatively cool palaeotemperatures (e.g. **Voigt et al., 2003**; **Wierzbowski and Joachimski, 2007**; **Rexfort and Mutterlose, 2009**; **Ullmann et al., 2014b**; **Sørensen et al., 2015**). In their low latitude compilation, **Prokoph et al. (2008)** addressed this issue by shifting all belemnite oxygen isotope data by 2.5 ‰ to match coeval brachiopod values. This isotopically heavy signature is compatible with a life style in which biomineralization in the surface waters does not occur or is of subordinate importance. Consequently, the LL raw data of **Prokoph et al. (2008)**, the IL compilation of **Dera et al. (2011)** and the new HL dataset from new Zealand, overlap entirely (**Fig.**

6) with LL average $\delta^{18}O$ values of up to +1.4 ‰ (Callovian). The use of belemnite oxygen isotope records for assessing global SST gradients is therefore problematic. Regional temperature changes throughout the Jurassic, however, seem to be well-captured by belemnite oxygen isotope ratios (e.g. **Dera et al., 2011**; **Korte and Hesselbo, 2011**; **Ullmann et al., 2014b** for Europe; **Stevens and Clayton, 1971** for New Zealand). Relative changes in belemnite oxygen isotope records may thus be taken to be of environmental significance.

For the Early and Middle Jurassic only few data are available from the Murihiku Terrane and no clear palaeoenvironmental conclusions can be drawn. For the Late Jurassic of New Zealand, **Stevens and Clayton (1971)**, **Podlaha et al. (1998)** and **Gröcke et al. (2003)** report a slight warming from the Oxfordian to Kimmeridgian. Such a climatic trend cannot be deduced from the mean values of the present study which do not differ significantly between middle Heterian (~late Oxfordian; -1.0 ± 0.8 ‰, 2err) and early Ohauan (~middle Kimmeridgian; -1.5 ± 0.7 ‰, 2err). A slight warming, however, is indicated by decreasing $\delta^{18}O$ maxima of the corresponding middle Heterian to lower Ohauan Substages (**Fig. 6**). Towards the end of the Jurassic $\delta^{18}O$ values increase to at most +1.6 ‰ in the Waikatoan Substage of the Puaroan Stage (~Late Tithonian), representing the highest values of the new record (**Fig. 6**). These values are heavier than those reported for northern IL of central Europe (**Jenkyns et al., 2002**), and are in excellent agreement with data reported by **Ditchfield (1997)** for the northern HL (Tordenskjoldberget Member of Svalbard ranging from the Tithonian to Valanginian Stages). Our new values for the latest Jurassic southern HL also resolve the problem of apparently asymmetric global temperature distribution with unproportionally warm southern HL suggested by **Gröcke et al. (2003)** for this interval, which appears to have been an artifact of sparse data availability. The subsequent warming through the Jurassic-Cretaceous boundary reported by **Gröcke et al. (2003)** is not visible in our new data due to the lacking coverage of this interval in the present study.

5.3 δ¹³C values

5.3.1 Permian-Triassic brachiopod data

The new HL Zealandian carbon isotope trend (**Fig. 7**) is compatible with the compiled record published by **Prokoph et al. (2008)**. The heaviest $\delta^{13}C$ values occur in the Permian and are taken to be related to globally high rates of organic carbon burial (**Berner, 2003, 2005**). The maximum in the early Late Permian Puruhauan (~ Wuchiapingian) Stage, however, seems to be ~10 Ma delayed with respect to the compilation of **Prokoph et al. (2008)** (**Fig. 7**). Values > +6 ‰ were found for Kungurian samples from the Australian Bowen Basin (**Korte et al., 2008**) and Tasmania (**Mii et al., 2012**), China (**Korte et al., 2005a**), Russia (**Grossman et al., 2008**), as well as the Kazanian of Spitsbergen (**Mii et al., 1997**) (see **Mii et al., 2013** for a compilation). The Puruhauan is currently regarded an informal unit whose distinct brachiopod fauna shows similarities with the Wuchiapingian faunas

of the Cherrabun Member in the Canning Basin (West Australia) (**Cooper, 2004**) and the Puruhauan is therefore assumed to represent the time equivalent of the Wuchiapingian. $\delta^{13}C$ values of the Puruhauan brachiopods are significantly more positive than those from the Cherrabun Member (**Korte et al., 2008**). The inclusion of the Echinalosia ovalis Zone in the previous Flettian Stage (**Cooper, 2004**) makes it unlikely that the Puruhauan localities are significantly older than Wuchiapingian/Capitanian, though (see brachiopod and bivalve zonal interpretations in **Korte et al., 2008** and **Waterhouse and Shi, 2013**). To decide, whether the very positive $\delta^{13}C$ values of the Puruhauan fossil localities are a local phenomenon or global in nature would require further assessment of the stratigraphic position of the Puruhauan strata.

The distinct carbon cycle perturbation associated with the Permian-Triassic mass extinction (see **Korte and Kozur, 2010** for a review), which is captured in organic matter in the Nelson area of New Zealand (**Krull et al., 2000**) is only poorly represented in our record (**Fig. 7**). This is due to lacking resolution, insufficient sample coverage and poor preservation in this critical interval.

The Kaihikuan (~ late Ladinian - Carnian) of Zealandia is characterized by relatively heavy $\delta^{13}C$ values, evidencing the recovery from the Permian-Triassic mass extinction. Zealandian values are on average 1.3 ± 0.3 ‰ (2err) heavier than reported for the LL (**Korte et al., 2005b**; **Prokoph et al., 2008**). This offset is also observed for the Otapirian (~Rhaetian) IL (New Caledonia), albeit smaller, amounting to 0.6 ± 0.4 ‰ (2err). A palaeolatitudinal reason for this effect is difficult to reconcile, since the positioning of the Zealandian terranes as well as their palaeogeographic situation are not unambiguously constrained to high precision (see e.g. reconstructions of **Stampfli and Borel, 2002**; **Scotese, 2004**; **Adams et al., 2007**; **Shi et al., 2010**; **Torsvik and Cocks, 2013**). Because there is no modern analogue for shelf areas in HL settings – probably even affected by the polar night– with comparable biotic activity it can only be speculated, how flora and fauna shaped the carbon cycle in the southern HL. Pronounced photosynthetic activity during the summers may have played a role for the comparatively heavy carbon isotope values of the investigated HL materials. Pronounced SST gradients could lead to heavier $\delta^{13}C$ signatures in high latitudes due to increasing fractionation factors between atmospheric CO_2 and DIC with decreasing temperature (**Zhang et al., 1995**). $\delta^{18}O$ values of high latitude calcite fossils (**Fig. 6**) contradict this mechanism, however, unless major contributions of freshwater led to isotopic depletion of the seawater $\delta^{18}O$ without altering its $\delta^{13}C$ signature. Furthermore, such a $\delta^{13}C$ gradient is not observed in modern oceans either (**GEOSECS, 1987**; **Marchal et al., 1998**). The evolution of the carbon isotope values throughout the Norian relies mostly on stable isotope measurements on bulk carbonate material (**Muttoni et al., 2004**; **Krystyn et al., 2007**; **Richoz et al., 2007**). Comparison of our southern HL brachiopod data with the tropical realm is therefore complicated. Nevertheless, a decreasing trend of bulk $\delta^{13}C$ values throughout the Norian has been observed by **Muttoni et al. (2004)**, albeit less pronounced than observed here and with lower absolute values.

5.3.2 Jurassic belemnite data

No apparent offset of carbonate isotope ratios between high and low latitudes is visible in the Jurassic. The absolute values of the new high latitude dataset are similar or lower than in the available compilations of **Prokoph et al. (2008)** and **Dera et al., (2011)** (see also **Stevens and Clayton, 1971**; **Podlaha et al., 1998**). Belemnite rostra tend to exhibit large intra-specimen heterogeneity of $\delta^{13}C$ values (e.g. **Wierzbowski and Joachimski, 2009**; **Sørensen et al., 2015**; **Ullmann et al., 2015**) and there is good indication for vital effects in some species (e.g. **Wierzbowski, 2002**; **Sørensen et al., 2015**). Relative offsets (or their absence) between the latitudinal realms might therefore be an effect of differing species assemblages (for an attempt at quantification, see **Prokoph et al., 2008**). Relative carbon isotope trends in belemnite rostra over long time spans, however, are found to reliably track changes in the global carbon cycle (e.g. **Dera et al., 2011**; **Korte and Hesselbo, 2011**; **Ullmann et al., 2015**).

$\delta^{13}C$ values show a decreasing trend throughout the Late Jurassic in all three latitudinal belts, including also the northern high latitudes (**Stevens and Clayton, 1971**; **Weissert and Mohr, 1996**; **Podlaha et al., 1998**; **Gröcke et al., 2003**; **Price and Rogov, 2009**). This long-term decrease is generally interpreted to be the result of changing global carbon cycle systematics from the Late Jurassic into the Early Cretaceous: The latter is thought to be characterized by a lower ratio of organic matter versus carbonate burial than the former, enriching carbon in the short-term carbon cycle in ^{12}C through time (**Weissert and Mohr, 1996**).

5.4 Sr/Ca ratios

The good agreement of $^{87}Sr/^{86}Sr$ ratios for the samples from the Murihiku, Brook Street, and Téremba Terranes with the seawater Sr isotope curve (**Fig. 5**) indicates that post-depositional effects on the measured Sr/Ca ratios are minor. Apart from diagenetic effects on Sr/Ca ratios in fossil materials, brachiopods have been found to show large inter-species variability in Sr/Ca ratios (**Brand et al., 2003**), thus complicating the direct interpretation of the observed significant brachiopod Sr/Ca changes throughout the Permian and Triassic (**Fig. 8**). The Sr/Ca ratios of Permian brachiopods reported here are in good agreement with Permian data of **Steuber and Veizer, (2002)**. The steep decrease in Sr/Ca ratios through the Middle-Late Triassic transition reported by **Steuber and Veizer (2002)**, however, is not supported by our new results. Carnian data of the **Steuber and Veizer (2002)** database that suggested a Middle to Late Triassic Sr/Ca decrease stem from the Western Carpathian Silická Brezová section and were subsequently interpreted to be affected by diagenesis (**Korte et al., 2005b**). The Late Triassic data reported here rather point to a significant increase in seawater Sr/Ca ratios from the Middle to Late Triassic and a subsequent decreasing trend that is reverted in the Late Norian (**Fig. 8**). Latest Triassic values observed here are again in good correspondence with the

results presented in **Steuber and Veizer (2002)**. Further data acquisition and cross-calibration with other methods for seawater reconstruction will be necessary to make a robust statement, if the indicated Late Triassic secular change in seawater Sr/Ca indeed took place, as also changing fossil assemblages can potentially lead to considerable changes in average observed Sr/Ca ratios (see data from **Brand et al., 2003**). The very limited Jurassic brachiopod data illustrate an intermediate position of brachiopod Sr/Ca ratios between lower oyster Sr/Ca and higher belemnite Sr/Ca ratios. This pattern is consistent with previous findings (**Voigt et al., 2003**; **Wierzbowski and Joachimski, 2007**; **Korte and Hesselbo, 2011**; **Ullmann et al., 2013a**) and indicates that the observed first order trends of Sr/Ca ratios in fossils through time is of palaeoenvironmental significance..

The newly analysed Sr/Ca ratios of Late Jurassic belemnites (*Belemnopsis* spp. and *Hibolithes* spp.) continue the belemnite- and oyster-derived Sr/Ca trend of **Ullmann et al. (2013a)** which runs broadly parallel to the seawater $^{87}Sr/^{86}Sr$ record as in the Early and Middle Jurassic. While in very good agreement with the data reported in **Ullmann et al. (2013a)**, the belemnite Sr/Ca ratios from **Podlaha et al. (1998)** are consistently lower than our Late Jurassic data.

Currently, absolute seawater Sr/Ca ratios cannot be unequivocally estimated from the Belemnopsis-Hibolithes assemblage, because no modern belemnite analogue with calcitic rostrum exists. Calibrations using other fossil groups could not be done for the interval investigated here due to lack of apprpriate material. Relative trends in the new data, however, indicate rising seawater Sr/Ca ratios from an absolute minimum in the Callovian-Oxfordian throughout the Late Jurassic, and a sharp decrease of ~15 %, preceding the Jurassic-Cretaceous transition.

6. CONCLUSIONS

Our new carbon and oxygen isotope data and Sr/Ca ratios from carbonate fossils of the Permian to Jurassic southern HL show significant, systematic variations.

Oxygen isotope ratios suggest a pronounced SST gradient in the Permian and possibly parts of the Jurassic, but comparatively warm HL in the Triassic. Carbon isotopes follow the general trends described for intermediate and low latitudes, further strengthening the global nature of secular variations in the global exogenic carbon cycle.

Newly reported brachiopod Sr/Ca data append the existing Permian database and fill a previously existing gap in the Late Triassic record. Brachiopod-based seawater Sr/Ca ratio estimates should be further calibrated to allow for a more robust estimate of seawater Sr/Ca ratios. Late Jurassic belemnite Sr/Ca ratios complete a Jurassic belemnite Sr/Ca curve, closely resembling the coeval global marine $^{87}Sr/^{86}Sr$ curve.

REFERENCES

Adams, C.J., Barley, M.E., Maas, R., Doyle, M.G., 2002. Provenance of Permian-Triassic volcaniclastic sedimentary terranes in New Zealand: Evidence from their radiogenic isotope characteristics and detrital mineral age patterns. New Zealand Journal of Geology and Geophysics 45 (2), 221-242. **doi: 10.1080/00288306.2002.9514970**.

Adams, C.J., Campbell, H.J., Griffin, W.L., 2007. Provenance comparisons of Permian to Jurassic tectonostratigraphic terranes in New Zealand: perspectives from detrital zircon age patterns. Geological Magazine 144 (4), 701-729.

Al-Aasm, I.S., Veizer, J., 1982. Chemical stabilization of low-Mg-calcite: An example of brachiopods. Journal of Sedimentary Petrology 52 (4), 1101-1109.

Almeida, M. J., Machado, J., Moura, G. Azevedo, M., Coimbra, J., 1998. Temporal and local variations in biochemical composition of *Crassostrea gigas* shells. Journal of Sea Research 40, 233–249.

Auclair, A.-C., Joachimski M.M., Lécuyer, C., 2003. Deciphering kinetic, metabolic and environmental controls on stable isotope fractionations between seawater and the shell of *Terebratalia transversa* (Brachiopoda). Chemical Geology 202, 59-78.

Berner, R.A., 2003. The long-term carbon cycle, fossil fuels and atmospheric composition. Nature 426, 323-326.

Berner, R.A., 2005. The carbon and sulfur cycles and atmospheric oxygen from middle Permian to middle Triassic. Geochimica et Cosmochimia Acta 69 (13), 3211-3217.

Brand, U., 1989. Biogeochemistry of Late Palaeozoic North American brachiopods and secular variation of seawater composition. Biogeochemistry 7, 159-193.

Brand, U., Veizer, J., 1980. Chemical diagenesis of a multicomponent carbonate system –1: Trace elements. Journal of Sedimentary Petrology 50 (4), 1219-1236.

Brand, U., Logan, A., Hiller, N., Richardson, J., 2003. Geochemistry of modern brachiopods: applications and implications for oceanography and palaeoceanography. Chemical Geology 198, 305-334.

Brayard, A., Bucher, H., Escarguel, G., Fluteau, F.,

Bourquin, S., Galfetti, T., 2006. The Early Triassic ammonoid recovery: Palaeoclimatic significance of diversity gradients. Palaeogeography, Palaeoclimatology, Palaeoecology 239, 374-395, **doi: 10.1016/j.palaeo.2006.02.003**.

Campbell, H.J., 1984. Petrography and metamorphism of the Teremba Group (Permian-Lower Triassic) and Baie de St.-Vincent Group (Upper Triassic-Lower Jurassic), New Caledonia. Journal of the Toyal Society of New Zealand 14 (4), 335-348. **doi:10.1080/03036758.1984.10421735**.

Campbell, H.J,. Grant-Mackie, J.A., 1984. Biostratigraphy of the Meozoic Baie de St.-Vincent Group, New Caledonia. Journal of the Royal Society of New Zealand 14 (4), 349-366. **doi:10.1080/03036758.1984.10421736**.

Campbell, H.J., Mortimer, N., Turnbull, I.M., 2003. Murihiku Supergroup, New Zealand: Redefined. Journal of the Royal Society of New Zealand 33 (1), 85-95.

Carpenter, S.J., Lohmann, K.C., 1995. $\delta^{18}O$ and $\delta^{13}C$ values of modern brachiopod shells. Geochimica et Cosmochimica Acta 59 (18), 3749-3764.

Chen, B., Joachimski, M.M., Shen, S.-Z., Lambert, L.L., Lai, X.-L., Wang, X.-D., Chen, J., Yuan, D.-X., 2013. Permian ice volume and paleoclimate history: Oxygen isotope proxies revisited. Gondwana Research 24, 77-89.

Cluzel, D., Maurizot, P., Collot, J., Sevin, B., 2012. An outline of the Geology of New Caledonia; from Permian-Mesozoic Southeast Gondwanaland active margin to Cenozoic obduction and supergene evolution. Episodes 35 (1), 72-86.

Coleman, M.L., Walsh, N.J., Benmore, R.A., 1989. Determination of both chemical and stable isotope composition in milligramme-size carbonate samples. Sedimentary Geology 65, 233-238.

Collot, J., Herzer, R., Lafoy, Y., Géli, L., 2009. Mesozoic history of the Fairway-Aotea Basin: Implications for the early stages of Gondwana fragmentation, Geochemistry, Geophysics, Geosystems 10 (12), Q12019, **doi:10.1029/2009GC002612**.

Compston, W., 1960. The carbon isotopic compositions of certain marine invertebrates and coals from the Australian Permian. Geochimica et Cosmochimica Acta 18, 1-22.

Cooper, R.A. (ed.), 2004. The New Zealand Geological Timescale, Institute of Geological and Nuclear Sciences Monograph 22, 284pp.

Cooper, A.F., Barreiro, B.A., Kimbrough, D.L., Mattinson, J.M., 1987. Lamprophyre dike intrusion and the age of the Alpine fault, New Zealand. Geology 15, 941-944.

Cúneo, N.R., Taylor, E.L., Taylor, T.N., Krings, M., 2003. In situ fossil forest from the upper Fremouw Formation (Triassic) of Antarctica: palaeoenvironmental setting and palaeoclimate analysis. Palaeogeography, Palaeoclimatology, Palaeoecology 197, 239-261. **doi:10.1016/S0031-0182(03)00468-1**.

Cusack, M., Pérez-Huerta, A., Chung, P., Parkinson, D., Dauphi, Y., Cuif, J.-P., 2008. Oxygen isotope equilibrium in brachiopod shell fibres in the context of biological control. Mineralogical Magazine 72 (1),

239-242.

Denison, R.E., Koepnick, R.B., Fletcher, A., Howell, M.W., Callaway, W.S., 1994. Criteria for the retention of original seawater $^{87}Sr/^{86}Sr$ in ancient shelf limestones. Chemical Geology 112, 131-143.

Dera, G., Brigaud, B,. Monna, F., Laffont, R., Pucéat, E., Deconinck, J.-F., Pellenard, P., Joachimski, M.M., Durlet, C., 2011. Climatic ups and downs in a disturbed Jurassic world. Geology 39, 215-218, **doi:10.1130/G31579.1**.

Ditchfield, P.W., 1997. High northern palaeolatitude Jurassic-Cretaceous palaeotemperature variation: new data from Kong Karls Land, Svalbard. Palaeogeography, Palaeoclimatology, Palaeoecology 130, 163-175.

GEOSECS, 1987. GEOSECS. Atlantic, Pacific, and Indian ocean expeditions, vol. 7: Shorebased data and graphics. International Decade of ocean Exploration. National Science Foundation.

Gradstein, F.M., Ogg, J.G., Schmitz, M., Ogg, G. (eds.), 2012,.The Geologic Time Scale 2012. Elsevier, 1176 p.

Grauvogel-Stamm, L., Ash, S.R., 2005. Recovery of the Triassic land flora from the end-Permian life crisis. Comptes Rendus Palevol 4, 593-608, **doi: 10.1016/j.crpv.2005.07.002**.

Gröcke, D.R., Price, G.D., Ruffell, A.H., Mutterlose, J., Baraboshkin, E., 2003. Isotopic evidence for Late Jurassic-Early Cretaceous climate change. Palaeogeography, Palaeoclimatology, Palaeoecology 202, 97-118.

Grossman, E.L., Yancey, T.E., Jones, T.E., Bruckschen, P., Chuvashov, B., Mazzullo, S.J., Mii, H.-S., 2008. Glaciation, aridification, and carbon sequestration in the Permo-Carboniferous: The isotopic record from low latitudes. Palaeogeography, Palaeoclimatology, Palaeoecology 268, 222-233.

Holland, M.M., Bitz, C.M., 2003. Polar amplification of climate change in coupled models. Climate Dynamics 21, 221-232, **doi:10.1007/s00382-003-0332-6**.

Horwitz, E.P., Chiarizia, R., Dietz, M.L., 1992. A novel strontium-selective extraction chromatographic resin. Solvent Extraction and Ion Exchange 10 (2), 313-336.

Howarth, R.J., McArthur, J.M., 1997. Statistics for strontium isotope stratigraphy. A robust LOWESS fit to the marine Sr-isotope curve for 0-206 Ma, with look-up table for the derivation of numerical age. Journal of Geology 105, 441-456.

Hudson, N., 2000. The Middle Jurassic of New Zealand, PhD thesis, University of Auckland, 333pp.

Hudson, N., 2003. Stratigraphy and correlation of the Ururoan and Temaikan Stage (Lower-Middle Jurassic, ?Sinemurian-Callovian) sequences, New Zealand. Journal of the Royal Society of New Zealand 33 (1), 109-147.

Imai, N., Terashima, S., Itoh, S., Ando, A., 1996. 1996 compilation of analytical data on nine GSJ geochemical reference samples, "sedimentary rock series". Geostandards Newsletter 20(2), 165–216.

Isbell, J.L., Henry, L.C., Gulbranson, E.L., Limarino, C.O., Fraiser, M.L., Koch, Z.J., Ciccioli, P.L., Dineen,

A.A., 2012. Glacial paradoxes during the late Paleozoic ice age: Evaluating the equilibrium line altitude as a control on glaciation. Gondwana Research 22, 1-19.

Jenkyns, H.C., Jones, C.E, Gröcke, D.R., Hesselbo, S.P, Parkinson, D.N., 2002. Chemostratigraphy of the Jurassic System: applications, limitations and implications for palaeoceanography. Journal of the Geological Society, London 159, 351-378.

Jones, C.E., Jenkyns, H.C., Hesselbo, S.P., 1994. Strontium isotopes in Early Jurassic seawater. Geochimica et Cosmochimica Acta 58, 1285–1301.

Kamp, P.J.J., Green, P.F., White, S.H., 1989. Fission track analysis reveals character of collisional tectonics in New Zealand. Tectonics 8 (2), 169-195. **doi:10.1029/TC008i002p00169**.

Kani, T., Hisanabe, C., Isozaki, Y., 2013. The Capitanian (Permian) minimum of $^{87}Sr/^{86}Sr$ ratio in the mid-Panthalassan paleo-atoll carbonates and its demise by the deglaciation and continental doming. Gondwana Research 24, 212-221.

Kear, D., Mortimer, N., 2003. Waipa Supergroup, New Zealand: a proposal. Journal of the Royal Society of New Zealand 33, 149-163.

Kidder, D.L., Worsley, T.R., 2004. Causes and consequences of extreme Permo-Triassic warming to globally equable climate and relation to the Permo-Triassic extinction and recovery. Palaeogeography, Palaeoclimatology, Palaeoecology 203, 207-237. **doi:10.1016/S0031-0182(03)00667-9**.

Korte, C., Kozur, H.W., 2010. Carbon-isotope stratigraphy across the Permian-Triassic boundary: A review. Journal of Asian Earth Sciences 39, 215-235. **doi:10.1016/j.jseas.2010.01.005**.

Korte, C, Hesselbo, S.P., 2011. Shallow marine carbon and oxygen isotope and elemental records indicate icehouse-greenhouse cycles during the Early Jurassic. Palaeoceanography 26, PA4219, **doi:10.1029/2011PA002160**.

Korte, C., Kozur, H.W., Bruckschen, P., Veizer, J., 2003. Strontium isotope evolution of Late Permian and Triassic seawater. Geochimica et Cosmochimica Acta 67, 47-62.

Korte, C., Jasper, T., Kozur, H.W., Veizer, J., 2005a. $\delta^{18}O$ and $\delta^{13}C$ of Permian brachiopods: a record of seawater evolution and continental glaciation. Palaeogeography, Palaeoclimatology, Palaeoecology 224, 333-351.

Korte, C., Kozur, H.W., Veizer, J., 2005b. $\delta^{13}C$ and $\delta^{18}O$ values of Triassic brachiopods and carbonate rocks as proxies for coeval seawater and palaeotemperature. Palaeogeography, Palaeoclimatology, Palaeoecology 226, 187-306.

Korte, C., Jasper, T., Kozur, H.W., Veizer, J., 2006. $^{87}Sr/^{86}Sr$ record of Permian seawater. Palaeogeography, Palaeoclimatology, Palaeoecology 240, 89-107.

Korte, C., Jones, P.J., Brand, U., Mertmann, D., Veizer, J, 2008. Oxygen isotope values from high-latitudes: Clues for Permian sea-surface temperature gradients and Late Palaeozoic deglaciation. Palaeogeography, Palaeoclimatology, Palaeoecology 269, 1-16.

Krull, E.D., Retallack, G.J., Campbell, H.J., Lyon, G.L.,

2000. $\delta^{13}C_{org}$ chemostratigraphy of the Permian-Triassic boundary in the Maitai Group, New Zealand: evidence for high-latitudinal methane release. New Zealand Journal of Geology and Geophysics 43, 21-32.

Krystyn, L., Bouquerel., H., Kuerschner, W., Richoz, S., Gallet, Y., 2007. Proposal for a candidate GSSP for the base of the Rhaetian Stage. New Mexico Museum of Natural History and Science Bulletin 41, 189-199.

Landis, C.A., Campbell, H.J., Aslund, T., Cawood, P.A., Douglas, A., Kimbrough, D.L., Pillai, D.D.L., Raine, J.I., Willsman, A., 1999. Permian-Jurassic strata at Productus Creek, Southland, New Zealand: implications for terrane dynamics of the eastern Gondwanaland margin. New Zealand Journal of Geology and Geophysics 42, 255-278.

Li, Q, McArthur, J.M. and Atkinson, T.C., 2012. Lower Jurassic belemnites as indicators of palaeotemperature. Palaeogeography, Palaeoclimatology, Palaeoecology 315-316, 38-45, **doi:10.1016/j.palaeo.2011.11.006**.

Limarino, C.O., Césari, S.N., Spalletti, L.A., Taboada, A.C., Isbell, J.L., Geuna, S., Gulbranson, E.L., 2014. A paleoclimatic review of southern South America during the late Paleozoic: A record from Icehouse to extreme greenhouse conditions. Gondwana Research 25, 1396-1421.

Marchal, O., Stocker, T.F., Joos, F., 1998. A latitude-depth, circulation-biogeochemical ocean model for paleoclimate studies. Development and sensitivities. Tellus 50B, 290-316.

McArthur, J.M., Howarth, R.J., Bailey, T.R., 2001. Strontium Isotope Stratigraphy: LOWESS Version 3: Best Fit to the Marine Sr-Isotope Curve for 0-509 Ma and Accompanying Look-up Table for Deriving Numerical Age. Journal of Geology 109, 155-170.

McArthur, J.M., Doyle, P., Leng, M.J., Reeves, K., Williams, C.T., Garcia-Sanchez, R., Howarth, R.J., 2007. Testing palaeo-environmental proxies in Jurassic belemnites: Mg/Ca, Sr/Ca, Na/Ca, $\delta^{18}O$ and $\delta^{13}C$. Palaeogeography, Palaeoclimatology, Palaeoecology 252, 464-480, **doi:10.1016/j.palaeo.2007.05.006**.

Mette, W., Elsler, A., Korte, C., 2012. Palaeoenvironmental changes in the Late Triassic (Rhaetian) of the Northern Calcareous Alps: Clues from stable isotopes and microfossils. Palaeogeography, Palaeoclimatology, Palaeoecology 350-352: 62-72. **doi:10.1016/j.palaeo.2012.06.013**.

Mii, H.-S., Grossman, E.L., Yancey, T.E., 1997. Stable carbon and oxygen isotope shifts in Permian seas of West Spitsbergen – global change or diagenetic artefact? Geology 25, 227-230.

Mii, H.-S., Shi, G.R., Cheng, C.-J., Chen, Y.-Y., 2012. Permian Gondwanaland paleoenvironment inferred from carbon and oxygen isotope records of brachiopod fossils from the Sydney Basin, southeast Australia. Chemical Geology 291, 87-103.

Mii, H.-S., Shi, G.R., Wang, C.-A., 2013. Late Paleozoic middle-latitude Gondwana environment-stable isotope records from Western Australia. Gondwana Research 24, 125-138.

Mortimer, N., 2004. New Zealand's Geological Founda-

tions. Gondwana Research 7 (1), 261-272.

Mortimer, N., Gans, P., Calvert, A., Walker, N., 1999. Geology and thermochronology of the east edge of the Median Batholith (Median Tectonic Zone): a new perspective on Permian to Cretaceous crustal growth of New Zealand. Island Arc 8, 404-425.

Mortimer, N., Rattenbury, M.S., King, P.R., Bland, K.J., Barrell, D.J.A., Bache, F., Begg, J.G., Campbell, H.J., Cox, S.C., Crampton, J.S., Edbrooke, S.W., Forsyth, P.J., Johnston, M.R., Jongens, R., Lee, J.M., Leonard, G.S., Raine, J.I., Skinner, D.N.B., Timm, C., Townsend, D.B., Tulloch, A.J., Turnbull, I.M., Turnbull, R.E., 20014. High-level stratigraphic scheme for New Zealand rocks. New Zealand Journal of Geology and Geophysics 57 (4). 402-419. **doi:10.1080/00288 306.2014.946062**.

Muttoni, G., Kent, D.V., Olsen, P.E., Di Stefano, P., Lowire, W., Bernasconi, S.M., Martín Hernández, F., 2004. Tethyan magnetostratigraphy from Pizzo Mondello (Sicily) and correlation to the Late Triassic Newark astrochronological polarity time scale. Geological Society of America Bulletin 116 (9), 1043-1058, **doi:10.1130/B25326.1**.

Nunn, E.V., Price, G.D., 2010. Late Jurassic (Kimmeridgian-Tithonian) stable isotopes (δ^{18}O, δ^{13}C) and Mg/Ca ratios: New palaeoclimate data from Helmsdale, northeast Scotland. Palaeogeography, Palaeoclimatology, Palaeoecology 292, 325-335, **doi:10.1016/j.palaeo.2010.04.015**.

Parkinson, D., Curry, G.B., Cusack, M., Fallick, A.E., 2005. Shell structure, patterns and trends of oxygen and carbon stable isotopes in modern brachiopods shells. Chemical Geology 219, 193-235.

Pole, M, 2009. Vegetation and climate of the New Zealand Jurassic. Journal of the Geological Society of Sweden 131, 105-111.

Podlaha, O.G., Mutterlose, J., Veizer, J., 1998. Preservation of δ^{18}O and δ^{13}C in belemnite rostra from the Jurassic/Early Cretaceous successions. American Journal of Science 298, 324-347.

Preto, N., Kustatscher, E., Wignall, P.W., 2010. Triassic climates – State of the art and perspectives. Palaeogeography, Palaeoclimatology, Palaeoecology 290, 1-10. **doi: 10.1016/j.palaeo.2010.03.015**.

Price, G.D., Mutterlose, J., 2004. Isotopic signals from late Jurassic-early Cretaceous (Volgian-Valanginian) sub-Arctic belemnites, Yatria River, Western Siberia. Journal of the Geological Society 161, 959-968.

Price, G.D., Rogov, M.A., 2009. An isotopic appraisal of the Late Jurassic greenhouse phase in the Russian Platform. Palaeogeography, Palaeoclimatology, Palaeoecology 273, 41-49.

Prokoph, A., Shields, G.A., Veizer, J., 2008. Compilation and time-series analysis of a marine carbonate δ^{18}O, δ^{13}C, ^{87}Sr/^{86}Sr and δ^{34}S database through Earth History. Geochimica et Cosmochimica Acta 87, 113-133.

Raine, J.I., Beu, A.G., Boyes, A.F., Campbell, H.J., Cooper, R.A., Crampton, J.S., Crundwell, M.P., Hollis, C.J., Morgans, H.E.G., 2015. Revised calibration of the New Zealand Geological Timescale: NZGT2015/1. GNS Science Report 2012/39, 53p.

Retallack, G.J., 2013. Permian and Triassic Greenhouse

crises. Gondwana Research 24, 90-103.

Retallack, G.J., Sheldon, N.D., Carr, P.F., Fanning, M., Thompson, C.A., Williams, M.L., Jones, B.G., Hutton, A., 2011. Multiple Early Triassic greenhouse crises impeded recovery from Late Permian mass extinction. Palaeogeography, Palaeoclimatology, Palaeoecology 308, 233-251.

Rexfort, A., Mutterlose, J., 2009. the role of biogeography and ecology on the isotope signature of cuttlefishes (Cephalopoda, Sepiidae) and the impact on belemnite studies. Palaeogeography, Palaeoclimatology, Palaeoecology 284, 153-163.

Richoz, S., Krystyn, L., Spötl, C., 2007. Towards a carbon isotope reference curve of the Upper Triassic. New Mexico Museum of Natural History and Science Bulletin 41, 366-367.

Scotese, C.R, 2004. A Continental Drift Flipbook. Journal of Geology 112, 729-741.

Sellwood, B.W., Valdes, P.J., 2006. Mesozoic climates: General circulation models and the rock record. Sedimentary Geology 190, 269-287. **doi: 10.1016/j. sedgeo.2006.05.013**.

Shaviv, N.J., Prokoph, A., Veizer, J., 2014. Is the Solar System's Galactic Motion Imprinted in the Phanerozoic Climate? Scientific Reports 4:6150, **doi: 10.1038/srep06150**.

Shi, G.R., Waterhouse, J.B., McLoughlin, S., 2010. The Lopingian of Australasia: a review of biostratigraphy, correlations, palaeogeography and palaeobiogeography. Geological Journal 45, 230-263, **doi: 10.1002/ gj.1213**.

Spandler, C., Worden, K., Arculus, R., Eggins, S., 2005. Igneous rocks of the Brook Street Terrane, New Zealand: Implications for Permian tectonics of eastern Gondwana and magma genesis in modern intra-oceanic volcanic arcs. New Zealand Journal of Geology and Geophysics 48, 167-183.

Spörli, K.B., 1978. Mesozoic tectonics, North Island, New Zealand. Geological Society of America Bulletin 89 (3), 415-425.

Spötl, C., Vennemann, T.W., 2003. Continuous-flow isotope ratio mass spectrometric analysis of carbonate materials. Rapid Communications in Mass Spectrometry 17, 1004-1006.

Stampfli, G.M., Borel, G.D., 2002. A plate tectonic model for the Palaeozoic and Mesozoic constrained by dynamic plate boundaries and restored synthetic oceanic isochrones. Earth and Planetary Science Letters 196, 17-33.

Steuber, T., Veizer, J., 2002. Phanerozoic record of plate tectonic control of seawater chemistry and carbonate sedimentation. Geology 30 (12), 1123-1126.

Stevens, G.R., 2008. Dactylioceratidae (Cephaloposa, Ammonoidea) from the Early Jurassic of New Zealand. New Zealand Journal of Geology and Geophysics 51, 317-330.

Stevens, G.R., Clayton, R.N., 1971. Oxygen isotope studies on Jurassic and Cretaceous belemnites from New Zealand and their biogeographic significance. New Zealand Journal of Geology and Geophysics 14 (4), 829-897.

Sutherland, R., 1999. Cenozoic bending of New Zealand

basement terranes and Alpine Fault displacement: A brief review. New Zealand Journal of Geology and Geophysics 42 (2), 295-301. **doi:10.1080/00288306 .1999.9514846**.

Sørensen, A.M., Ullmann, C.V., Thibault, N., Korte, C., 2015. Geochemical signatures of the early Campanian belemnite Belemnellocamax mammillatus from the Kristianstad Basin in Scania, Sweden. Palaeogeography, Palaeoclimatology, Palaeoecology 433, 191-200.

Taylor, E.L., Taylor, T.N., 1993. Fossil Tree Rings and Palaeoclimate from the Triassic of Antarctica. In: Lucas, S.G, Morales, M. (eds.): The Non-marine Triassic. New Mexico Museum of Natural History & Science Bulletin No. 3, pp. 453-455.

Torsvik, T.H., Cocks, L.R.M., 2013. Gondwana from top to base in space and time. Gondwana Research 24, 999-1030.

Trotter, J.A., Williams, I.S., Nicora, A., Mazza, M., Rigo, M., 2015. Long-term cycles of Triassic climate change: a new δ18O record from conodont apatite. Earth and Planetary Science Letters 415, 165-174.

Turnbull, I.M., Allibone, A.H. (compilers) (2003). Geology of the Murihiku area: scale 1:250,000. Lower Hutt: Institute of Geological & Nuclear Sciences Limited. Institute of Geological & Nucelar Science 1:250,000 geological map 20. 74p. + 1 folded map.

Ullmann, C.V., Korte, C., 2015. Diagenetic alteration in low-Mg calcite from macrofossils: a review. Geological Quarterly 59 (1), 3-20.

Ullmann, C.V., Hesselbo, S.P., Korte, C., 2013a. Tectonic forcing of Early to Middle Jurassic seawater Sr/Ca, Geology 41 (12), 1211-1214.

Ullmann, C.V., Campbell, H.J., Frei, R., Hesselbo, S.P., Pogge von Strandmann, P.A.E., Korte, C., 2013b. Partial diagenetic overprint of Late Jurassic belemnites from New Zealand: Implications for the preservation potential of δ7Li values in calcite fossils. Geochimica et Cosmochimica Acta 120, 80-96, **doi: 10.1016/j. gca.2013.06.029**.

Ullmann, C.V., Campbell, H.J., Frei, R., Korte, C., 2014a. Geochemical signatures in Late Triassic brachiopods from New Caledonia. New Zealand Journal of Geology and Geophysics 57 (4), 420-431.

Ullmann, C.V., Thibault, N., Ruhl, M., Hesselbo, S.P., Korte, C., 2014b. Effect of a Jurassic oceanic anoxic event on belemnite ecology and evolution. PNAS 111 (28), 10073-10076.

Vander Putten, E., Dehairs, F., Keppens, E., Baeyens, W., 2000. High resolution distribution of trace elements in the calcite shell layer of modern Mytilus edulis: Environmental and biological controls. Geochimica et Cosmochimica Acta 64 (6), 997–1011.

Veizer, J., Fritz, P., Jones, B., 1986. Geochemistry of brachiopods: Oxygen and carbon isotopic records of Palaeozoic oceans. Geochimica et Cosmochimica Acta 50, 1679-1696.

Veizer, J., Ala, D., Azmy, K., Bruckschen, P., Buhl, D., Bruhn, F., Carden, G.A.F., Diener, A., Ebneth, S., Godderis, Y., Jasper, T., Korte, C., Pawellek, F., Podlaha, O.G., Strauss, H., 1999. 87Sr/86Sr, δ13C and δ18O evolution of Phanerozoic seawater. Chemical Geology 161, 59-88, **doi:10.1016/S0009-2541(99)00081-9**.

Voigt, S., Wilmsen, M., Mortimore, R.N., Voigt, T., 2003. Cenomanian palaeotemperatures derived from the oxygen isotopic composition of brachiopods and belemnites: evaluation of Cretaceous palaeotemperature proxies. International Journal of Earth Sciences 92, 285-299.

Waterhouse, J.B., Shi, G.R., 2013. Climatic implications from the sequential changes in diversity and biogeographic affinities of brachiopods and bivalves in the Permian of eastern Australia and New Zealand. Gondwana Research 24, 139-147.

Weissert, H., Mohr, H., 1996. Late Jurassic climate and its impact on carbon cycling. Palaeogeography, Palaeclimatology, Palaeoecology 122, 27-43.

Wierzbowski, H., 2002. Detailed oxygen and carbon isotope stratigraphy of the Oxfordian in Central Poland. International Journal of Earth Sciences 91, 304-314. **doi:10.1007/s005310100217**.

Wierzbowski, H., Joachimski, M., 2007. Reconstruction of late Bajocian-Bathonian marine palaeoenvironments using carbon and oxygen isotope ratios of calcareous fossils from the Polish Jura Chain (central Poland). Palaeogeography, Palaeoclimatology, Palaeoecology 254, 523-540.

Wierzbowski, H., Joachimski, M.M., 2009. Stable isotopes, elemental distribution, and growth rings of belemnopsid belemnite rostra: proxies for belemnite life habitat. Palaios 24, 377-386. **doi:10.2110/palo.2008. p08-101r**.

Yamamoto, K., Asami, R., Iryu, Y., 2010. Within-shell variations in carbon and oxygen isotope compositions of two modern brachiopods from a subtropical shelf environment off Amami-o-shima, southwestern Japan, Geochemistry Geophysics Geosystems 11, Q10009, **doi:10.1029/2010GC003190**.

Zakharov, Y.D., Sha, J., Popov, A.M., Safronov, P.P., Shorochova, S., Volynets, E.B., Biakov, A.S., Burago, V.I., Zimina, V.G., Konovalova, I.V., 2009. Permian to earliest Cretaceous climatic oscillations in the eastern Asian continental margin (Sikhote-Alin area), as indicated by fossils and isotope data. GFF 131, 25-47.

Zhang, J., Quay, P.D., Wilbur, D.O., 1995. Carbon isotope fractionation during gas-water exchange and dissolution of CO2. Geochimica et Cosmochimica Acta 59 (1), 107-114.

Zharkov, M.A., Chumakov, N.M., 2001. Palaeogeography and Sedimentation Settings during Permian-Triassic Reorganizations in Biosphere. Stratigraphy and Geological Correlation 9 (4), 340-363.